

# Beyond maps: Patterns of formation processes at the Middle Pleistocene open-air site of Marathousa 1, Megalopolis Basin, Greece

D. Giusti<sup>a,\*</sup>, V. Tourloukis<sup>a</sup>, G. E. Konidaris<sup>a</sup>, N. Thompson<sup>a</sup>, P. Karkanas<sup>c</sup>,  
E. Panagopoulou<sup>d</sup>, K. Harvati<sup>a</sup>

<sup>a</sup>*Paläoanthropologie, Senckenberg Centre for Human Evolution and Palaeoenvironment, Eberhard Karls Universität Tübingen, Rümelinstr. 23, 72070 Tübingen, Germany*

<sup>b</sup>*Friedrich-Alexander University of Erlangen-Nürnberg, Institute of Prehistory and Early History, Kochstr. 4/18, 90154 Erlangen, Germany*

<sup>c</sup>*Malcolm H. Wiener Laboratory for Archaeological Science, American School of Classical Studies at Athens, Greece*

<sup>d</sup>*Ephoreia of Palaeoanthropology-Speleology of Greece, Athens, Greece*

---

## Abstract

Recent excavations at the Middle Pleistocene open-air site of Marathousa 1 have unearthed in one of the two investigated areas (Area A) a partial skeleton of a single individual of *Elephas (Palaeoloxodon) antiquus* and other faunal remains in spatial and stratigraphic association with lithic artefacts. In Area B, a much higher number of lithic artefacts was collected, spatially and stratigraphically associated with other faunal remains. The two areas are stratigraphically correlated, the main fossiliferous layers representing an *en masse* depositional process in a lake margin context. Evidence of butchering (cut-marks) has been identified on two bones of the elephant skeleton, as well on other mammal bones from Area B. However, due to the secondary deposition of the main find-bearing units, it is of primary importance to evaluate the degree and reliability of the spatial association of the lithic artefacts with the faunal remains. Indeed, spatial correlation does not necessarily imply causation: natural syn- and post-depositional processes may equally produce spatial association. Assessing the extent of the post-depositional reworking processes is crucial to fully comprehend the archaeological record, and therefore to reliably interpret past human behaviours. The present

---

\*Corresponding author

Email address: domenico.giusti@uni-tuebingen.de (D. Giusti)

study uses a comprehensive set of spatial statistics in order to disentangle the depositional processes behind the distribution of the archaeological and palaeontological record at Marathousa 1. Results of our analyses suggest minor reworking and substantial spatial association of the lithic and faunal assemblages, supporting the current interpretation of Marathousa 1 as a butchering site.

*Keywords:* Spatial taphonomy, Site formation processes, Vertical distribution, Fabric analysis, Point pattern analysis, Middle Pleistocene

---

**1 1. Introduction**

2 The analysis of archaeological site formation processes, intensively studied since  
3 the early 1970s ([Isaac, 1967](#); [Schiffer, 1972, 1983, 1987](#); [Shackley, 1978](#); [Wood and](#)  
4 [Johnson, 1978](#); [Schick, 1984, 1986, 1987](#); [Petraglia and Nash, 1987](#); [Petraglia and](#)  
5 [Potts, 1994](#), among others), is nowadays fully integrated in the archaeological practice  
6 ([????Malinsky-Buller et al., 2011](#); [Vaquero et al., 2012](#); [Bargalló et al., 2016](#), among  
7 others). Drawing inferences about past human behaviours from scatters of archaeological  
8 remains must account for syn-depositional and post-depositional contextual  
9 processes.

10 Several methods are currently applied in order to qualify and quantify the type and  
11 degree of reworking of archaeological assemblages. Within the framework of a geoar-  
12 chaeological and taphonomic approach, spatial statistics offer meaningful contributions  
13 in unravelling site formation and modification processes from spatial patterns.

14 The present study uses a comprehensive set of multiscale spatial statistics in order  
15 to disentangle the depositional processes behind the spatial distribution of the archaeo-  
16 logical and palaeontological record recovered during excavation at the Middle Pleis-  
17 tocene open-air site of Marathousa 1, Megalopolis, Greece ([Panagopoulou et al., 2015](#);  
18 [Harvati et al., 2016](#)).

19 Section 2 introduces the site and specifies the main aims of this work. This section  
20 1 set out our theoretical framework by offering a overview of spatial statistic methods  
21 and presenting the rationale behind our spatial taphonomic approach.

22 The study of the clast fabric (dip and strike of elongated sedimentary particles,

23 including bones and artefacts), first addressed by Isaac (1967); Bar-Yosef and Tch-  
24 ernov (1972); Schick (1986), has more recently been found to successfully discrimi-  
25 nate between sedimentary processes (Bertran and Texier, 1995; Bertran et al., 1997),  
26 leading to a noteworthy development of methods and propagation of applications in  
27 Palaeolithic site formation studies (Lenoble and Bertran, 2004; Lenoble et al., 2008;  
28 McPherron, 2005; Benito-Calvo et al., 2009, 2011; Benito-Calvo and de la Torre,  
29 Bernatchez, 2010; Boschian and Saccà, 2010; Domínguez-Rodrigo et al., 2012;  
30 Domínguez-Rodrigo and García-Pérez, 2013; Domínguez-Rodrigo et al., 2014c; de la  
31 Torre and Benito-Calvo, 2013; Walter and Trauth, 2013; García-Moreno et al., 2016;  
32 Sánchez-Romero et al., 2016, among others).

33 The vertical distribution of materials, on the other hand, has been long investigated  
34 with the aim of identifying cultural levels, by visually interpreting virtual profiles (but  
35 see Anderson and Burke (2008) for a quantitative approach).

36 However, archaeological horizons may be subject to vertical rearrangement by syn-  
37 and post-depositional processes. Several experimental studies, for example, have in-  
38 vestigated the effect of trampling on the vertical displacement of artefacts (Villa and  
39 Courtin, 1983; Gifford-Gonzalez et al., 1985; Nielsen, 1991; Eren et al., 2010). Al-  
40 though these works have reported a negative correlation between artefact size and ver-  
41 tical displacement, particle size sorting of lithic assemblages, when exposed to phys-  
42 ical geomorphic agents (such as gravity, water flow, waves and tides, wind), has been  
43 widely documented (Rick, 1976; Schick, 1986; Petraglia and Nash, 1987; Morton,  
44 2004; Lenoble, 2005; Bertran et al., 2012).

45 Bone and lithic refitting analysis is an additional, particularly robust method in  
46 investigating the stratigraphic integrity of a site (Villa, 1982, 1990; Todd and Stanford,  
47 1992; Morin et al., 2005; Sisk and Shea, 2008). Furthermore, bone and lithic refits  
48 have been shown to provide reliable clues about the spatio-temporal dimension of past  
49 human behaviours, by discriminating activity areas (López-Ortega et al., 2011, 2015;  
50 Vaquero et al., 2012, 2015; Clark, 2016; Gabucio et al., 2017).

51 Finally, distribution maps are cornerstones of the archaeological documentation  
52 process and are primary analytic tools. However, their visual interpretation is prone to  
53 subjectivity and is not reproducible (Bevan et al., 2013). Since the early 1970's (see

54 Hodder and Orton (1976); Orton (1982) and references therein), the traditional, intuitive,  
55 ‘eyeballing’ method of spotting spatial patterns has been abandoned in favour  
56 of more objective approaches, extensively borrowed from other fields. Nevertheless,  
57 quantitative methods, while still percolating in the archaeological sciences from neighbouring  
58 disciplines, are not extensively used. Moreover, only a relatively small number  
59 of studies have explicitly applied spatial point pattern analysis or geostatistics to the  
60 study of site formation and modification processes (Lenoble et al. (2008); Domínguez-  
61 Rodrigo et al. (2014b,a, 2017); Carrer (2015); Giusti and Arzarello (2016); Organista  
62 et al. (2017) - but see Hivernel and Hodder (1984) for an earlier work on the subject).

63 The goal of a taphonomic approach to spatial analysis is to move beyond distribution  
64 maps by applying a comprehensive set of multiscale and multivariate spatial  
65 statistics in order to reliably construct inferences from spatial patterns. An exhaustive  
66 spatial analytic approach to archaeological inference, combined with a taphonomic  
67 perspective, is essential for evaluating the accumulation process and integrity of the ar-  
68 chaeological assemblage, and consequently for a reliable interpretation of past human  
69 behaviours.

## 70 2. Marathousa 1

71 The site (Fig. 1), discovered in 2013 at the edge of an active lignite quarry (Thompson  
72 et al., this issue), is located between lignite seams II and III in the Pleistocene de-  
73 posits of the Megalopolis basin, Marathousa Member of the Choremi Formation (van  
74 Vugt et al., 2000). The regular alternation of lacustrine clay, silt and sand beds with  
75 lignite seams has been interpreted having cyclic glacial (or stadial) and interglacial (or  
76 interstadial) origin (Nickel et al., 1996). The half-graben configuration of the basin,  
77 with major subsidence along the NW-SE trending normal faults along the eastern mar-  
78 gin, resulted in the gentle dip of the lake bottom at the opposite, western, margin of the  
79 lake, enabling the formation of swamps and the accumulation of organic material for  
80 prolonged periods of time (van Vugt et al., 2000).

81 Two excavation areas have been investigated since 2013: Area A, where several  
82 skeletal elements of a single individual of *Elephas (Palaeoloxodon) antiquus* have been

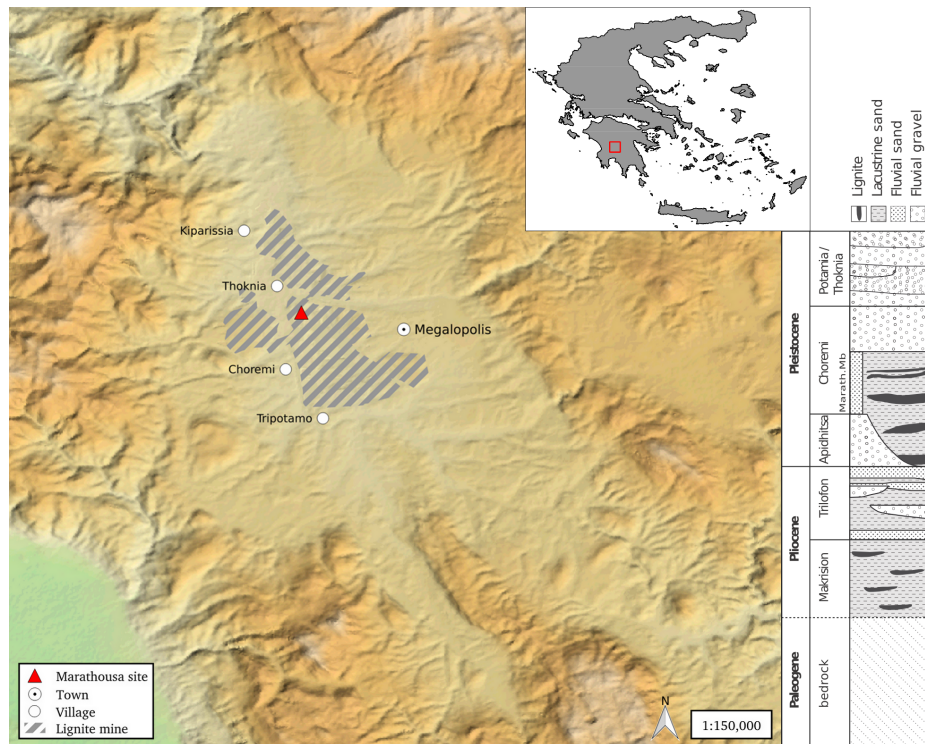


Figure 1: Geographical location of the Marathousa 1 site in the Megalopolis basin and stratigraphic column, modified after [van Vugt et al. \(2000\)](#).

83 unearthened, together with a number of lithic artefacts (Konidaris et al., this issue; Tour-  
84 loukis et al., this issue); and Area B, located 60 m to the South along the exposed  
85 section, where the lithic assemblage is richer and occurs in association with a faunal  
86 assemblage composed of isolated elephant bones, cervids and carnivores among others  
87 (Fig. ??). Evidence of butchering (cut-marks) have been identified on two of the ele-  
88 phant bones from Area A, as well on elephant and other mammal bones from Area B  
89 (Konidaris et al., this issue).

90 An erosional contact separates the two main find-bearing units in both areas, namely  
91 UA3c/4 and UB4c/5a (Fig. 3). In Area A, the elephant remains lie at the contact of  
92 UA3c/4 and are covered by UA3c; while in Area B, most of the remains were collected  
93 from unit UB4c. For both areas, the working hypothesis is that the flow event repre-  
94 sented by units UA3c and UB4c eroded and scoured the exposed surface (where the  
95 elephant was lying), thereby entraining clastic material (including probably artefacts)  
96 and re-depositing this material at a close distance (see Karkanas et al., this issue).

97 The erosional event described above, and specifically the erosional contacts be-  
98 tween the fossiliferous horizons in the two areas, provide the essential background for  
99 the analysis and interpretation of the spatial distributions at Marathousa 1.

100 The secondary depositional nature of the main find horizons raises the question  
101 of how reliable is the spatial association between the lithic artefacts and the partial  
102 skeleton of a single *Elephas (Palaeoloxodon) antiquus* individual and other faunal  
103 remains. Since spatial association does not necessarily imply causation, and conse-  
104 quently synchrony (??), the answer has important consequences for the interpretation  
105 of the site in the broader context of the Middle Pleistocene human-proboscidean inter-  
106 actions. We aim to tackle this question and disentangle the formation processes acting  
107 at Marathousa 1 on the basis of spatial patterns through a three-prong spatial analytic  
108 approach:

- 109 1. by analysing, in a frame of references, the fabric of remains from relevant strati-  
110 graphic units;
- 111 2. by quantifying and comparing their relative vertical distributions;
- 112 3. by identifying spatial trends in either the assemblage intensities and the associa-

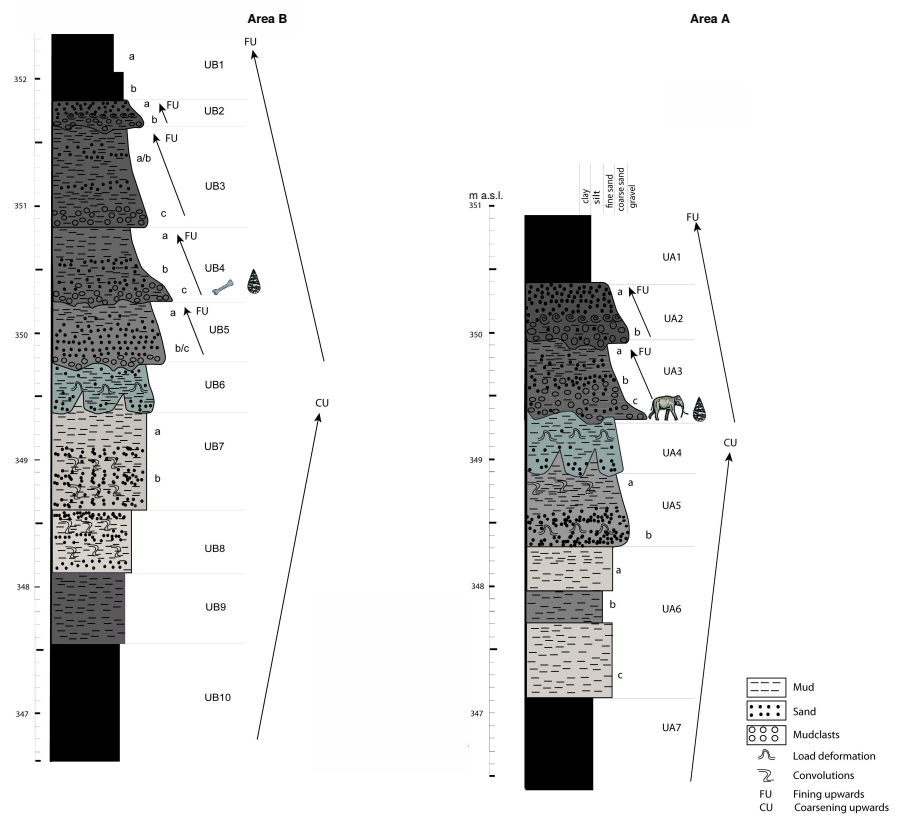


Figure 2: Stratigraphic setting of the Marathousa 1 site, modified after Karkanas et al. (this issue).

113 tions between classes of remains.

114 **3. Material and methods**

115 Since 2013, systematic investigation of the Marathousa 1 site has been carried out  
116 by a joint team from the Ephoreia of Palaeoanthropology-Speleology (Greek Ministry  
117 of Culture) and the University of Tübingen. A grid system of 1 square meter units  
118 was set up, oriented -14 degrees off the magnetic North, and including the two areas  
119 of investigation. The excavation of the deposit proceeded in 50x50 cm sub-squares  
120 in Area B and 1x1 m squares in Area A, and spits of 5 to 10 cm thickness, respec-  
121 tively. Systematic water-screening of sediments was carried out on-site using 1 mm  
122 sieves in order to guarantee recovery of the small-size fraction (e.g., micro-artefacts,  
123 small mammal remains, fish, molluscs and small fragments of organic and inorganic  
124 material). The three-dimensional coordinates of finds (i.e., all the lithic artefacts, teeth  
125 and diagnostic bones; bones and organic material with a-axis  $\geq$  20 mm), collected  
126 spits of sediment, samples and geological features (e.g., erosional contacts and mud  
127 cracks) were recorded with a Total Station. Dense clouds of surface points of the Ele-  
128 phant skeletal elements were acquired using both a Total Station and a close-range  
129 photogrammetric technique. The dimensions (length, width and thickness) of regis-  
130 tered finds were measured on-site with millimetre rules. Orientation (dip and strike) of  
131 elongated particles (i.e., faunal remains, large wood fragments and lithic artefacts) was  
132 recorded since 2013 with a 30 degree accuracy, using a clock-like system (the strike  
133 was measured, relatively to the grid North, in twelve clockwise intervals). In 2015,  
134 the use of a compass and inclinometer with an accuracy of 1 degree was introduced in  
135 Area B to gradually replace the former method. Strike (azimuth) and dip measurements  
136 were taken along the symmetrical longitudinal a-axis (SLA) of the bones ([Domínguez-](#)  
137 [Rodrigo and García-Pérez, 2013](#)), the lithic artefacts ([Bertran and Texier, 1995](#)) and  
138 organic material, using the lowest endpoint of the axis as an indicator of the vector  
139 direction.

140 The present study focuses on the excavated stratigraphic units in which most of the  
141 archaeological and palaeontological remains were recovered in both excavation areas,

namely in UA3c and UA4 in Area A, and UB4c and UB5a in Area B. From the total, subset samples of material were used for each specific spatial analysis. For the fabric analysis we included material collected until 2016. For the vertical distribution and point pattern analyses, the region of investigation was limited to the squares excavated from 2013 until 2015, 25 and 29 square meters respectively in each area.

The analyses were performed in R statistical software ([R Core Team, 2016](#)). In order to make this research reproducible ([Marwick, 2017](#)), a repository containing a compendium of data, source code and text is open licensed and available at the DOI: [10.5281/zenodo.822273](https://doi.org/10.5281/zenodo.822273)

### *3.1. Fabric analysis*

Comparative fabric analysis was conducted with the aim to investigate the dynamics of the depositional processes at Marathousa 1. The analysis of the orientation of elongated clasts can distinguish three main types of pattern (isotropic, planar and linear fabric), each associated with different sedimentary processes.

At the margin of a lacustrine environment, relatively close to the surrounding relief, a combination of high- and low-energy processes can be expected. According to the depositional context of the site (Karkanas et al., this issue), a strong preferred orientation of clasts (linear pattern) would suggest the action of massive slope processes such as mudslides and debris / hyperconcentrated flows. On the other hand, whereas the frontal lobes of debris flows have been found to show a more random orientation (isotropic pattern), overland flows have been associated with planar fabrics ([Lenoble and Bertran, 2004](#)). Conversely, in a lacustrine floodplain, anisotropy without significant transport can be caused by low-energy processes such as lake transgression and regression, as well as water-sheet flows formed during rainy seasons. Isotropic patterns have been observed in different parts of mudflats as well ([Cobo-Sánchez et al., 2014](#)).

Nevertheless, grey zones exist between different depositional processes, so that an unequivocal discrimination based only on fabric observations is often not possible, and other taphonomic criteria must also be considered () .

Since fabric strength has been found to be positively correlated with the shape and size of the clast, for the fabric analysis we subset samples of remains with length

Table 1: List of sampled observations for the fabric analysis.

Sample	<i>n</i>	Type		
		Fauna	Wood	Lithic
UA3c	49	23	25	1
UA4	38	8	30	-
<i>E. (P.) antiquus</i>	63			
UB4c (clock)	86	68	4	14
UB4c (compass)	65	47	10	8

<sup>172</sup>  $\geq 2$  cm and elongation index (the ratio length/width)  $I_e \geq 1.6$  ([Lenoble and Bertran, 2004](#)). The samples are listed in Table 1 and include mostly wood fragments and faunal remains from the four stratigraphic units under investigation. No distinction of skeletal elements was made, both due to the high fragmentation rate of faunal remains in Area B, and because recent experiments showed a similar orientation pattern for different bone shapes ([Domínguez-Rodrigo and García-Pérez, 2013](#); [Domínguez-Rodrigo et al., 2012](#)).

<sup>179</sup> The sample of bones belonging to the individual of *Elephas (P.) antiquus* from <sup>180</sup> Area A was analysed separately and included the humerus, ulna, femur and tibia; the <sup>181</sup> atlas, axis and 16 complete vertebrae or vertebral fragments; 29 complete ribs or rib <sup>182</sup> fragments; 2 calcanea; 4 metatarsals/metacarpals; the pyramidal; the trapezoid and the <sup>183</sup> pelvis. The sample from UB5a was too small (only 7 observations) and was therefore <sup>184</sup> excluded. The sample from the UB4c unit was divided in two sub-samples considered <sup>185</sup> separately: those recorded using the clock method and those recorded using the <sup>186</sup> compass method. All the sampled observations are representative of the whole study <sup>187</sup> area.

<sup>188</sup> Rose diagrams and uniformity tests, such as Rayleigh, Kuiper, Watson and Rao <sup>189</sup> tests ([Jammalamadaka et al., 2001](#)), were used to visualise and evaluate circular isotropy <sup>190</sup> in the sample distribution. The Rayleigh test is used to assess the significance of the <sup>191</sup> sample mean resultant length ( $\bar{R}$ ), assuming that the distribution is unimodal and not <sup>192</sup> bi- or plurimodal. The  $\bar{R}$  ranges from 0 to 1: values close to 1 indicate that the data are <sup>193</sup> closely clustered around the mean direction; when the data are evenly spread  $\bar{R}$  has a

194 value close to 0. A *p* – *value* lower than 0.05 rejects the hypothesis of randomness with  
195 a 95% confidence interval. Kuiper, Watson and Rao are omnibus tests used to detect  
196 multimodal departures from circular uniformity. All of them were applied using a sig-  
197 nificance level of *alpha* = 0.01. The test results were evaluated against critical values:  
198 a result higher than the critical value rejects the null hypothesis of isotropy with a 99%  
199 confidence interval.

200 Randomness testing of three-dimensional data was conducted with the Woodcock  
201  $S_1/S_3$  test ([Woodcock and Naylor, 1983](#)). Considering both the dip (plunge) and strike  
202 (bearing) of the oriented items, this method, based on three ordered eigenvalues ( $S_1$ ,  
203  $S_2$ ,  $S_3$ ), is able to discriminate the shape and strength of the distributions. The shape  
204 parameter  $K = \frac{\ln(S_1/S_2)}{\ln(S_2/S_3)}$  ranges from zero (uni-axial girdles) to infinite (uni-axial clus-  
205 ters). The parameter  $C = \ln(S_1/S_3)$  expresses the strength of the preferential orien-  
206 tation, and its significance is evaluated against critical values from simulated random  
207 samples of different sizes. A perfect random uniform distribution would have  $C = 0$   
208 and  $K = 1$ .

209 The Benn ([Benn, 1994](#)) diagram adds to the Woodcock test an isotropy ( $IS =$   
210  $S_3/S_1$ ) and an elongation ( $ES = 1 - (S_2/S_1)$ ) index. Like the former method, it is  
211 able to differentiate between linear (cluster), planar (girdle) or isotropic distributions.  
212 There are no published raw data from actualistic studies on depositional processes af-  
213 fecting the orientation of bones and artefacts deposited on lacustrine floodplains (but  
214 see [Morton \(2004\)](#) and [Cobo-Sánchez et al. \(2014\)](#) as pioneer studies on this subject).  
215 However, we included in the Benn diagram references to published results from obser-  
216 vation of fabrics in modern subaereal slope deposits ([Bertran et al., 1997; Lenoble and](#)  
217 [Bertran, 2004](#)).

218 Fabric analysis is a powerful tool but, as suggested by [Lenoble and Bertran \(2004\)](#),  
219 it is not sufficient to unequivocally discriminate processes and should therefore be in-  
220 tegrated with the analysis of other diagnostic features.

221 *3.2. Vertical distribution*

222 We provisionally assume that a general concentration of unsorted material in the  
223 proximity of the erosional surfaces would support an autochthonous origin of the as-

Table 2: List of sampled observations for the vertical distribution and point pattern analyses.

Sample	<i>n</i>	Lithic class					Faunal class			
		Debris/chip	Flake	Bone flake	Tool	Core	Indet.	Bone	Tooth	Microfauna
UA3c	279	46	2	-	1	-	1	171	14	44
UA4	61	3	1	-	-	-	-	45	4	8
UB4c	1243	753	154	1	34	6	2	246	28	19
UB5a	101	50	12	-	3	-	-	30	3	3

224 semblages ; whereas a poorly to extremely poorly sorted and homogeneous vertical dis-  
 225 tribution of remains from the UA3c and UB4c units would suggest an allochthonous  
 226 origin and a subsequent redeposition triggered by a massive process, e.g., debris or  
 227 hyperconcentrated flows. Graded bedding could result in such fluid depositional envi-  
 228 ronments, associated with a decrease in transport energy.

229 In order to estimate the degree of vertical dispersion while controlling for the size  
 230 of the archaeological material, dimensional classes were set up following typological  
 231 criteria. Lithic artefacts were classified as debris/chips when smaller than a cutoff  
 232 length of 15 mm (see Tourloukis et al., this issue). Other classes include flakes, tools  
 233 and cores; the latter being the bigger and heavier debitage product. Table 2 summarises  
 234 the sample size for each class. Lithic debris/chips constitutes the larger part of the  
 235 assemblages from UB4c (60%) and UB5a (49%); whereas in Area A it represents only  
 236 a moderate percentage in the upper UA3c unit (16%). The very rare presence of lithic  
 237 artefacts in the underlying unit UA4 is nevertheless significant. In this unit, the faunal  
 238 remains are also found in much lower numbers, their number reduced to one fourth  
 239 of those found in UA3c. For the point pattern analysis (see below), we used the same  
 240 subset of materials for both excavation areas.

241 For Area B, the material recovered from the water-screening was randomly prove-  
 242 nanced according to the 5 cm depth of the excavated spit and the coordinates of the  
 243 50x50 cm quadrant of the excavation square. Following the same excavation protocol,  
 244 the same procedure was applied for the water-screened material of Area A, which was  
 245 randomly provenanced according to 3D-coordinates of the 1x1 m excavation square  
 246 and 10 cm spit.

247 Inverse-distance weighting (IDW) interpolation of the recorded points of contact  
248 between the UB4c/5a and UA3c/4 stratigraphic units were used to reconstruct their  
249 erosional surfaces, in Areas A and B, respectively (Fig. 3a,b). IDW assumes spatial  
250 autocorrelation and calculates, from a set of irregular known points, weighted aver-  
251 age values of unknown points. Thus, in order to address our specific objective, i.e., to  
252 quantify and analyse the vertical distribution of the archaeological and palaeontologi-  
253 cal material, we measured the minimum orthogonal distance of each specimen to the  
254 interpolated erosional surface (Fig. 3c).

255 For the units above and below this surface (i.e., UB4c and UB5a), the relative  
256 distribution of lithic classes and faunal remains was informally tested by means of  
257 kernel density estimations. Likewise, in Area A the relative vertical distribution of  
258 remains from UA3c was estimated relative to the absolute elevation of the elephant  
259 remains and the range of elevations of the UA3c/4 surface. Finally, a Student's two  
260 sample t-test allowed us to compare the empirical distributions of different groups of  
261 remains for each stratigraphic unit.

262 *3.3. Point pattern analysis*

263 A spatial point pattern is defined as the outcome of a random spatial point process  
264 (repetitions of it would always create a different pattern). The observed patterns of the  
265 archaeological and palaeontological remains were treated as manifestations of spatial  
266 point processes, i.e., site formation processes. Point pattern analysis investigates the  
267 spatial arrangement of points with the aim of identifying spatial trends. In order to  
268 integrate the previous studies of the fabric and vertical distributions, we directed our  
269 point pattern analysis equally to the intensity of the patterns (the rate of occurrence of  
270 the recorded finds) and to the spatial interaction between different types of finds.

271 As the average number of random points per unit area, intensity informs about ho-  
272 mogeneity or inhomogeneity in the distribution of events generated by a point process,  
273 i.e., whether the rate of occurrence is uniform or spatially varying across the study area.  
274 Intensity, usually non-parametrically evaluated by means of kernel density estimation  
275 (Diggle, 1985), was assessed for the distribution of material from the UB4c, UB5a  
276 and UA3c units. Cross-validation bandwidth, which assumes a Cox process, and edge

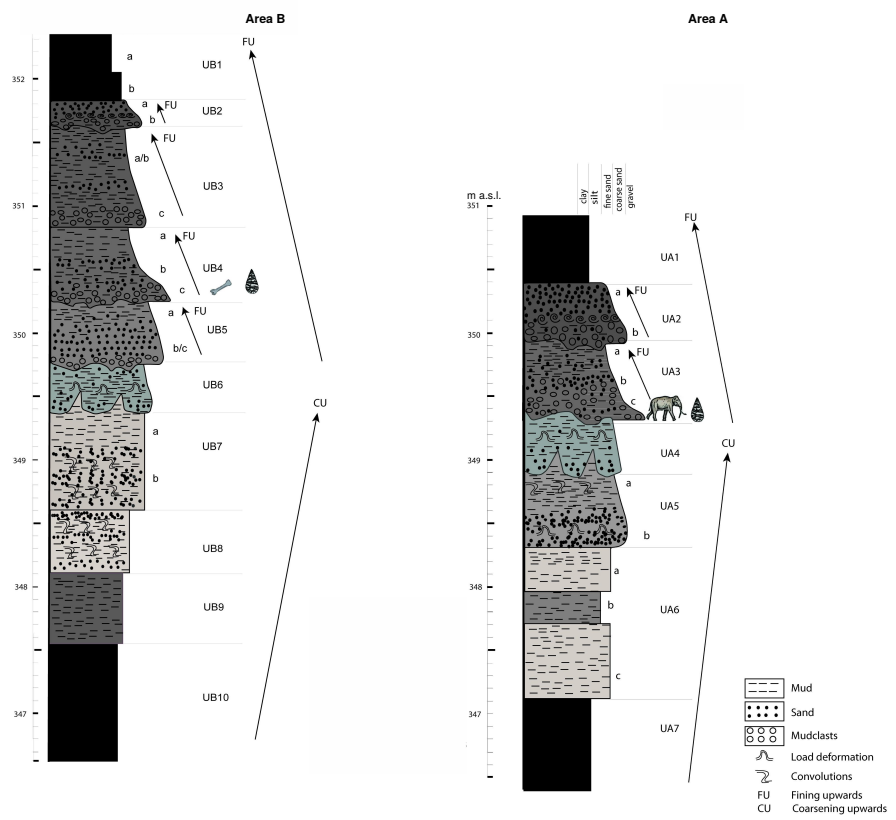


Figure 3: IDW interpolation of the UA3c/4 (a) and UB4c/5a (b) points of erosional contact; the color scale denotes elevation a.s.l. Illustration of the method used to quantify the vertical dispersion of remains with respect to the UB4c/5a surface (c).

277 correction were applied using the methods described in [Diggle \(1985\)](#).

278 In the presence of a covariate, it is recommended to further investigate the depen-  
279 dence of intensity on that explanatory variable. In order to evaluate whether variation  
280 in the density of materials was correlated to the topography of the erosional surface,  
281 we computed a local likelihood smoothing estimate of the intensity of remains from  
282 UB4c as a function of the UB4c/5a surface elevation model ([Baddeley et al., 2012](#)).  
283 Formal tests enabled us to assess the evidence of that dependence and to quantify the  
284 strength of the covariate. The Kolmogorov-Smirnov test of CSR (Complete Spatial  
285 Randomness) and Berman's  $Z_2$  statistics were used to test the strength of evidence for  
286 a covariate effect. The Receiver Operating Characteristic (ROC) plot, and the area  
287 under the ROC curve (AUC), closely related to Berman's  $Z_2$  test, measure the magni-  
288 tude of the covariate effect. AUC values close to 1 or 0 indicate strong discrimination,  
289 whereas intermediate values (0.5) suggest no discrimination power.

290 Whereas intensity is a first-order property of the point process, multiscale inter-  
291 point interaction is measured by second or higher-order moment quantities, such as  
292 the Ripley's  $K$  correlation function ([Ripley, 1976, 1977](#)) and the distance  $G$ -,  $F$ - and  
293  $J$ -functions. Three different types of inter-point interaction are possible: random, reg-  
294 ular or cluster. Regular patterns are assumed to be the result of inhibition processes,  
295 while cluster patterns are the result of attraction processes. In order to reduce the  
296 edge effect bias in estimating the correlation between points, we implemented Rip-  
297 ley's isotropic edge correction ([Ohser, 1983; Ripley, 1988](#)). In a hypothesis-testing  
298 framework, pointwise envelopes were computed by 199 random simulations of the  
299 null hypothesis. Thus, values of the empirical distribution (black solid line) were plot-  
300 ted against the benchmark value (red dotted line) and the envelopes (grey area) which  
301 specify the critical points for a Monte Carlo test ([Ripley, 1981](#)).

302 In order to test the spatial dependence between remains associated with the ero-  
303 sional event of UB4c and those associated with the underlying UB5a unit, we treated  
304 the data as a multivariate point pattern, assuming that the point patterns in UB4c and  
305 UB5a are expressions of two different stationary point processes, i.e., depositional  
306 events. We performed a cross-type pair correlation function ( $g_{ij}(r)$ ), derivative of the  
307 multitype  $K_{ij}(r)$  function, which is the expected number of points of type  $j$  lying at a

308 distance  $r$  of a typical point of type  $i$ . The function is a multiscale measurement of the  
309 spatial dependence between types  $i$  (UB4c) and  $j$  (UB5a). Randomly shifting each of  
310 the two patterns, independently of each other, estimated values of  $\hat{g}_{ij}(r)$  are compared  
311 to a benchmark value  $g_{ij}(r) = 1$ , which is consistent with independence or at least with  
312 lack of correlation between the two point processes.

313 In addition to the pair correlation function, the multitype nearest-neighbour  $G_{ij}(r)$   
314 function was used to estimate the cumulative distribution of the distance from a point of  
315 type  $i$  (UB4c) to the nearest point of type  $j$  (UB5a). It measures the spatial association  
316 between the two assemblages. For the cross-type  $G$ -function, the null hypothesis states  
317 that the points of type  $j$  follow a Poisson (random) distribution in addition to being  
318 independent of the points of type  $i$ . Thus, in a randomisation technique, when the solid  
319 line of the observed distribution ( $\hat{G}_{ij}(r)$ ) is above or below the shaded grey area, the  
320 pattern is significantly consistent with clustering or segregation, respectively. Complete  
321 spatial randomness and independence (CSRI) of the two point processes would support  
322 an exogenous origin hypothesis for the assemblage recovered from the UB4c unit. On  
323 the other hand, positive or negative association can be interpreted as expression of  
324 different endogenous processes.

325 The particle size spatial distribution of the lithic assemblage from UB4c was inves-  
326 tigated by means of a transformation of the multitype  $K$ -function ( $K_{i\bullet}(r) - K(r)$ , see  
327 [Baddeley et al. \(2015\)](#), p.608). In this case, we treated the data as the manifestation of a  
328 single multitype point process. In a joint distribution analysis, the locations and types  
329 of points are assumed to be generated at the same time. The null model of a random  
330 labelling test states that the type of each point is determined at random, independently  
331 of other points, with fixed probabilities. The estimated  $K$ -function for a subset of pos-  
332 sible combinations was evaluated against the envelope of Monte Carlo permutations of  
333 the class of remains. Likewise with the vertical distribution, a horizontal clustering of  
334 small specimens, such as lithic debris/chips, together with larger dimensional classes  
335 of remains would suggest the lack of sorting by natural depositional processes and a *en*  
336 *mass* model of deposition.

337 As for the three-dimensional distribution of the lithic artefacts in Area A, and their  
338 spatial association with the partial skeleton of the *E. (P.) antiquus*, we applied three-

dimensional univariate and bivariate second-order functions. A rectangular box of 20 square meters and 80 cm vertical extent was selected for the analyses (green outline in Fig. 9a). Assuming homogeneity, the univariate pair correlation function ( $g_3(r)$ ) was estimated for the pattern of all the artefacts (mostly debris/chips) from UA3c and UA4. In the specific context of the site, complete spatial randomness (CSR) would suggest that the pattern most probably is the result of a random distribution process, such as a high energy mass movement. In contrast, other natural processes would produce clustering or segregation of the lithic artefacts. Spatial aggregation, if not generated by obstructions, would support an *in situ* primary origin of the assemblage.

In support to the pair correlation function, the cross-type nearest-neighbour function has been applied in order to compute, for each artefact recovered from the UA3c and UA4 units, the nearest point associated with the elephant skeleton. A prevalence of short distances would indicate aggregation of the lithic artefacts around the mass of the elephant; whereas a uniform or symmetric distribution would support random independent processes.

## 4. Results

### 4.1. Fabric analysis

The rose diagrams in Fig. 4 visualise the circular distributions of the examined specimens. Overall, the UA4 sample and the sample of elephant bones show predominant peaks in the NE quadrant; while the ones from units UA3c and UB4c suggest uniform to multimodal distributions. Specifically, the UA4 sample distribution (Fig. 4b) spreads largely in the NE quadrant. Similarly, the circular distribution of the elephant sample (Fig. 4c), mainly lying in UA4, resembles the former distribution: it is skewed to the SW and concentrated in the NE quadrant. On the other hand, the UA3c sample (Fig. 4a) and the two samples from Area B (Fig. 4d,e) suggest a different isotropic scenario.

Table 3 summarises the results of the circular uniformity tests. With regard to the UA3c sample, the Rayleigh test ( $p - value = 0.029$ ) rejected the null hypothesis of circular uniformity. The mean resultant length ( $\bar{R} = 0.268$ ) and the mean direction

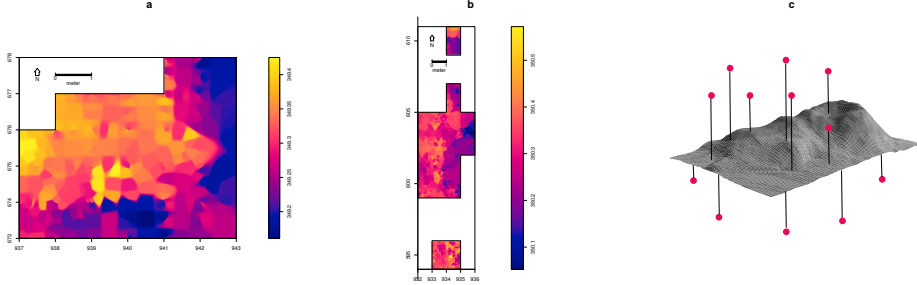


Figure 4: Rose diagrams showing the bearing patterns of samples from UA3c (a), UA4 (b), the elephant carcass (c) and UB4c (d: clock method, e: compass method)

Table 3: Global tests for circular uniformity

Sample	mean dir.	Rayleigh		Kuiper		Watson		Rao		level
		$\bar{R}$	p - value	test	critical value	test	critical value	test	critical value	
UA3c	77.17°	0.268	0.029	2.4698	2.001	0.2967	0.267	271.8367	160.53	0.01
UA4	35.79°	0.386	0.003	2.5656	2.001	0.3437	0.267	246.3158	163.73	0.01
<i>E. (P.) antiquus</i>	54.64°	0.489	2.775e-07	3.4811	2.001	0.906	0.267	291.4286	155.49	0.01
UB4c (clock)	83.96°	0.167	0.091	2.327	2.001	0.2466	0.267	309.7674	155.49	0.01
UB4c (compass)	128.14°	0.225	0.037	1.6917	2.001	0.1862	0.267	153.3846	155.49	0.01

of 77.17° are thus significant, assuming the distribution is unimodal. However, the Kuiper, Watson and Rao omnibus tests also rejected the null hypothesis of uniformity, therefore suggesting multimodal anisotropy in the distribution, as shown by the rose diagram (Fig. 4a).

For the UA4 sample and the subset of elephant bones, all the tests agreed in rejecting the null hypothesis in favour of a preferentially oriented distribution. The Elephant sample, with respect to the other, showed stronger anisotropy and significantly higher  $\bar{R}$ . As suggested by the rose diagrams (Fig. 4c), this sample has a mean direction towards the NE (55°) and relatively low circular variance (29°).

The UB4c sub-samples had discordant test results when considering the Rayleigh and the omnibus statistics. According to the Rayleigh test, the mean resultant length ( $\bar{R}$ ) and the mean direction were not significant for the sub-sample of measurements recorded with the clock system. Conversely, a weak significant test result was obtained for the sub-sample of measurements recorded using the compass. Overall, for the latter sub-sample all the omnibus tests suggested significant isotropy (Fig. 4e). On the other

383 hand, the Kuiper and Rao tests, suggested a multimodal departure from uniformity for  
384 the sample recorded using the clock method (Fig. 4d).

385 The results obtained for the UA3c sample and the UB4c sub-sample recorded using  
386 the clock method are most probably due to the shape of those distributions. Indeed, the  
387 clock system, being less accurate, tends to produce a less dense distribution, more  
388 subject to show a multimodal shape when the distribution is actually uniform (Fig. 4a,  
389 d).

390 The Woodcock eigenvalues ratio graph (Fig. 5a) presents the shape ( $K$ ) and strength  
391 ( $C$ ) of the distributions. Fig. 5b plots confidence levels of Monte-Carlo critical  $C$  val-  
392 ues, varying for sample sizes. The two samples from Area B, together with the UA3c  
393 sample, having low  $C$  values, plotted close to the origin of the ratio graph. Thus, they  
394 suggest nearly significant randomness. On the other hand, the UA4 and the elephant  
395 samples, with higher  $C$  values, showed a stronger and significant tendency to orient  
396 preferentially. The shape parameter  $K$  of the samples varied from  $K = 0.7$  for the  
397 UB4c sample measured with the compass to  $K = 0.1$  for the elephant sample. Overall,  
398 all the samples plotted below the average shape value ( $K = 1$ ) between girdles and  
399 clusters distributions.

400 The Benn diagram (Fig. 6) resembles the Woodcock ratio graph (Fig. 5a). The  
401 samples from units UB4c and UA3c clearly plotted at a distance from the UA4 and the  
402 elephant samples. The UB4c sub-sample of measurements recorded with the compass,  
403 together with the UA3c sample, plotted in the centre of the ternary graph. As shown  
404 above, the UB4c sub-sample of measurements taken using the clock system exhibited  
405 more isotropy.

406 Compared to the ranges recorded for modern natural processes (debris flow, runoff,  
407 solifluction), the fabric from the UA3c and UB4c units plotted well inside the cluster of  
408 debris flows, with the UB4c (clock) sample suggesting even more random orientations.  
409 On the other hand, the sample of elephant remains, which lie mostly on UA4 and are  
410 covered by UA3c, plotted significantly close to the sample from unit UA4. They both  
411 presented the lowest isotropy index ( $IS$ ), but not high elongation index ( $EL$ ). Thus,  
412 they plotted in the average between linear and planar orientations, within the range of  
413 runoff processes. Yet they still plotted at the margins of the cluster of debris flows

.../artwork/Fig5\_.pdf

Figure 5: Woodcock's eigenvalues ratio graph (a) and plot of the Monte-Carlo critical  $S_1/S_3$  test values, for varying sample sizes and confidence levels (b), modified from [Woodcock and Naylor \(1983\)](#).

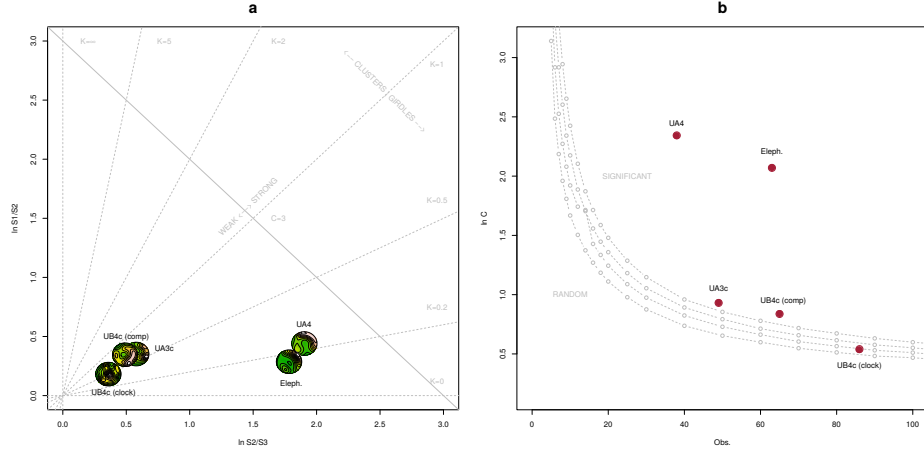


Figure 6: Benn's diagram. Fabric ranges of natural processes modified from Bertran et al. (1997); Lenoble and Bertran (2004).

414 fabrics. Moreover, the elephant sample showed a more planar attitude with respect to  
415 the UA4 sample.

#### 416 4.2. Vertical distribution

417 Fig. 7 compares the distribution of the absolute elevations of the partial skeleton  
418 of the *Elephas (P.) antiquus* with the other remains from Area A. Overall, the vertical  
419 distribution of the elephant approximates a normal distribution with mean ( $\mu$ ) 349.25 m  
420 a.s.l. and standard deviation ( $\sigma$ ) 0.12 m. The mean elevation of the erosional contact  
421 between the two stratigraphic units is slightly above the latter ( $\mu = 349.30$  m). Al-  
422 though difficult to quantify due to its mixed nature, the range of elevations of this con-  
423 tact, as estimated from the IDW interpolation (Fig. 3a), is relatively small ( $\sigma = 0.06$  m).

424 Three lithic artefacts (two flakes and one tool) from the UA3c unit are located  
425 within its positive half. Only one flake has been found in the lower UA4, at about  
426 349.10 m, together with three chips. However, they plotted well within the left tail  
427 of the debris/chip distribution from the unit above. Despite the scarcity ofdebitage  
428 products in this area, waste products (debris/chip) are relatively well represented (16%  
429 of the UA3c sample). Their vertical distribution approximates a normal distribution  
430 ( $\mu = 349.50$  m and  $\sigma = 0.18$  m), having almost 50% of the sample in the range of

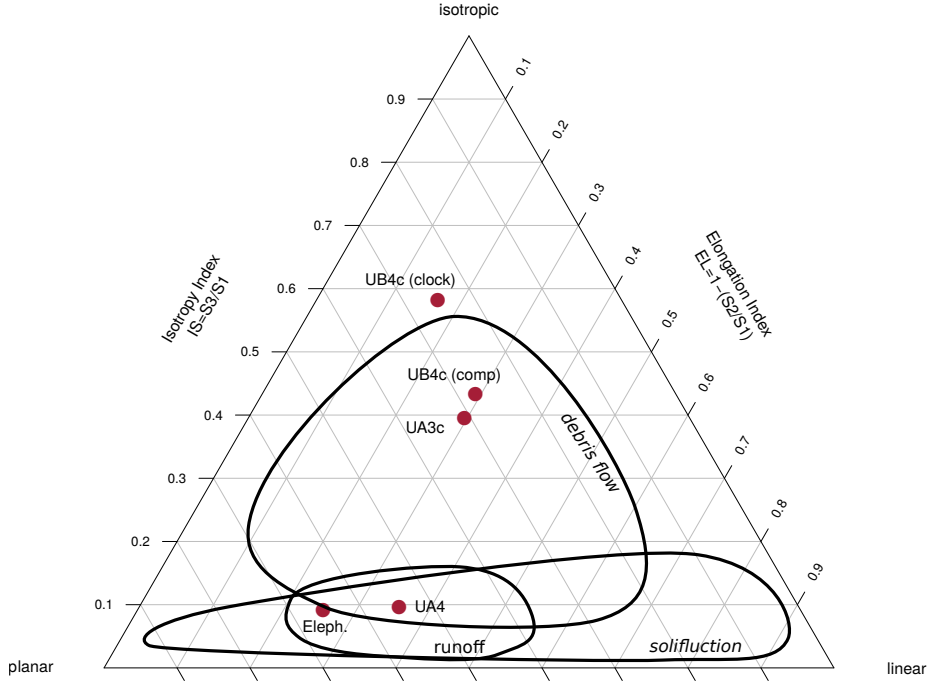


Figure 7: Empirical density functions of absolute elevations (meters a.s.l.) of remains from Area A. The histogram represents the *Elephas (P.) antiquus* range of elevations; the grey area shades the  $Q_3 - Q_1$  range of the erosional UA3c/4 surface; dashed lines indicate mean values.

elevations of the erosional surface and the rest above it. Notably, the distribution of the faunal remains from the same unit resembles that of the debris/chip. The Welch two sample t-test ( $p - value = 0.5099$ ) failed to reject the null hypothesis that the two population means are equal. On the other hand, the vertical distribution of faunal remains recovered from the UA4 unit is comparable with that of the *Elephas* ( $p - value = 0.6562$ ). Nevertheless, the density functions altogether clearly confirm one of the main observations assessed during excavation, namely that the elephant remains and most of the recovered faunal and lithic material in Area A lie at or close to the UA3c/4 contact, with unit UA3c covering the remains.

Fig. 8 shows the empirical density functions of the minimum distances from each specimen from Area B to the UB4c/5a erosional contact (Fig. 3b). The combined distribution of any type of find from the UB5a unit (Fig. 8a) skewed to the left with

443 a short tail (up to -0.3 m). The mode, between 5 and 10 cm below the roof of UB5a,  
444 indicates a general concentration of material very close to the contact of this unit with  
445 the overlying UB4c, in accordance with the mean distribution of the different classes of  
446 remains. Although the majority of both the lithic and faunal assemblages were found  
447 in the uppermost 15 cm of UB5a, few debris/chips and bone fragments occur lower  
448 in the sequence, yet no more than 30 cm below the roof of this unit. Very few flakes,  
449 three tools and no cores have been found in this unit. As a whole, the lithic assemblage  
450 from UB5a, mostly composed by debris/chips, is only 7% of the most conspicuous  
451 assemblage from UB4c.

452 The global distribution of unit UB4c was right skewed (up to almost 0.6 m) and cen-  
453 tered at about 5 cm above the contact with the underlying unit UB5a (Fig. 8b). Almost  
454 30% of the sample fell exactly at the erosional contact that separates UB4c from UB5a.  
455 The density estimations of the lithic debris/chip, flakes, tools and faunal remains sig-  
456 nificantly overlap, whereas the distribution of the six cores shows a bimodal shape with  
457 peaks at 5 and 20 cm above the contact. However, the Welch Two Sample t-test of the  
458 lithic and faunal sample means failed to reject the null hypothesis ( $p$ -value = 0.6295).

#### 459 4.3. Point pattern analysis

460 Results of the point pattern analysis are complementary to those obtained from the  
461 analysis of the vertical and fabric distributions.

462 Regarding Area A, kernel density estimation and three-dimensional functions were  
463 applied in order to quantitatively depict the spatial distribution of the lithic assemblage  
464 in relation to the elephant skeleton.

465 Fig. 9a shows the smoothing kernel intensity estimation of the combined lithic and  
466 faunal assemblage from the UA3c unit. Contour lines delimit the density of the lithic  
467 sample. The partial skeleton of the *E. (P.) antiquus* is superimposed on it. A pre-  
468 liminary visual examination of the plot suggests a homogeneous distribution of lithics  
469 (mostly debris/chips) and fossils. Spots of higher density appear to be spread around  
470 and in association with the elephant remains.

471 The univariate pair correlation function of the joined lithic assemblage from the  
472 UA3c and UA4 units (Fig. 9b) suggests aggregation of finds. The estimated  $\hat{g}_3(r)$

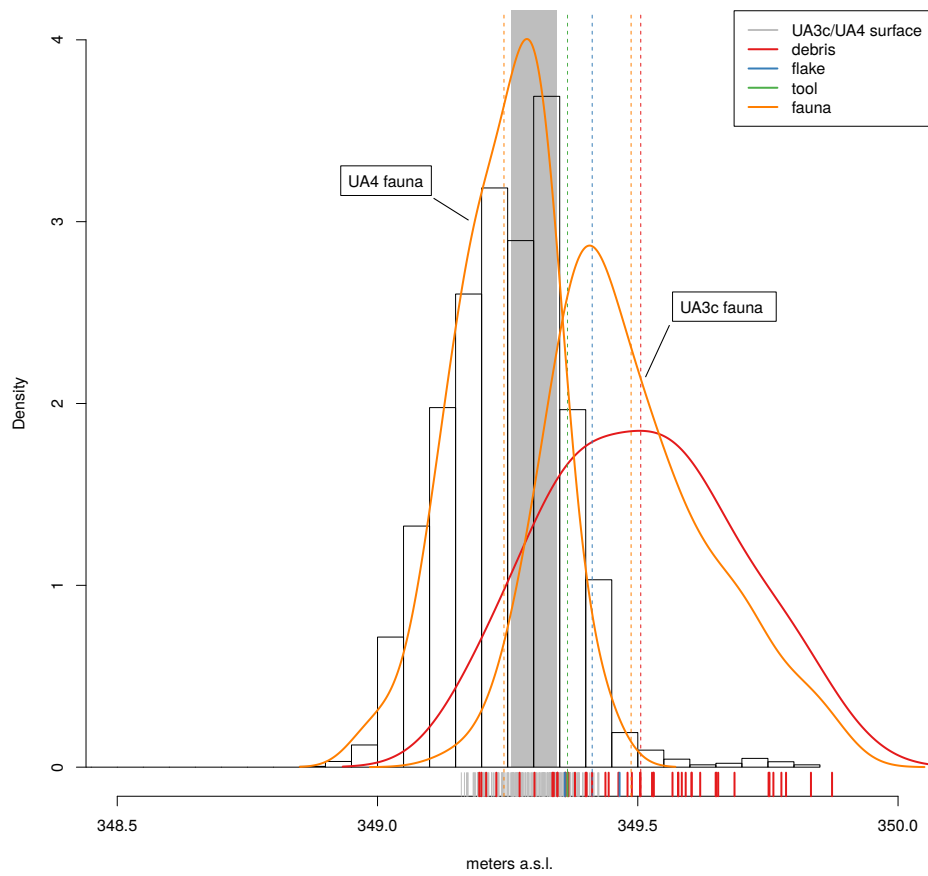


Figure 8: Empirical density functions of minimum orthogonal distances ( $d$ ) to the UB4c/5a surface. The histogram represents the total distribution of remains from UB5a (a) and UB4c (b); dashed lines indicate mean values.

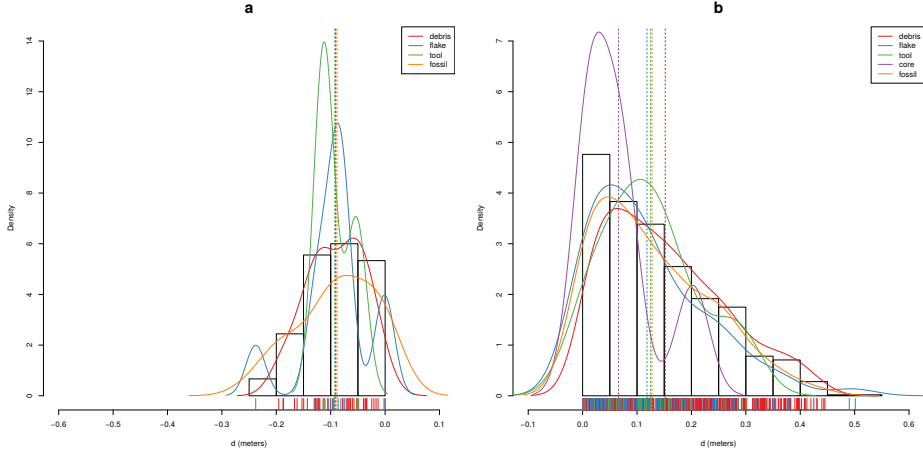


Figure 9: Kernel smoothed intensity function of the lithic and faunal assemblages from UA3c. Isolines mark the density of the lithic artefacts (a). Pair correlation function ( $g_3(r)$ ) of a three-dimensional pattern of lithic artefacts from UA3c and UA4. Grey envelope of 999 Monte Carlo simulations under the CSR null hypothesis (b). Three-dimensional distance from each lithic artefact from UA3c and UA4 to the nearest neighbour elephant remain (c).

473 function (black solid line) wanders above the benchmark value (red dotted line) until  
 474 values of  $r = 0.8$ . However, for distances between 35 and 65 cm, it lies above the  
 475 grey envelope of significance for the null hypothesis of CSR, indicating that at those  
 476 distances artefacts occur closer than expected in the case of random processes. For  
 477 values of  $r > 0.8$ , the function stabilises at values close to 0, suggesting a Poisson  
 478 distribution. The plot illustrates the random distribution of finds between patches of  
 479 clusters that we observe in the kernel density estimation (Fig. 9a).

480 The histogram in Fig. 9c shows the density of the distances calculated from each  
 481 artefact to the nearest-neighbour elephant remain. A right skewed distribution, with  
 482 a prevalent peak at 10 cm and mean  $\mu \approx 30$  cm is an indication of the relatively strong  
 483 aggregation of events around the mass of the elephant skeleton.

484 As for Area B, the analysis first focused on the spatial distribution and cross-  
 485 correlation of the assemblages from UB4c and UB5a (Fig. 10); and secondly on the  
 486 interaction between classes of remains from UB4c (Fig. 11).

487 Figs. 10a,b respectively show kernel density estimations of the combined lithic and

488 faunal assemblages from both the units analysed. Despite the samples size difference,  
489 a first visual examination suggests the presence of interesting spatial structures.

490 Regarding the UB4c unit (Fig. 10a), the high density of material concentrated  
491 around the western square 934/600 suggests that the pattern could have been the re-  
492 sult of an inhomogeneous, non-uniform depositional process. Visual comparison of  
493 the density plot with the elevation model of the erosional contact between the UB4c  
494 and UB5a units (Fig. 3b) suggests positive correlation between lower elevations (topo-  
495 graphic depressions) and higher density of remains. Fig. 10c shows the results of the  
496  $\rho$ -function, which estimates the intensity of the UB4c sample assemblage as a func-  
497 tion of the covariate underlying topography created by the erosional event. Within the  
498 range of elevation between 350.2 and 350.4 m, the occurrence of finds is higher and  
499 the intensity decreases with the rise of elevation, i.e., finds are more likely to be found  
500 at lower elevations than would be expected if the intensity was constant.

501 Spatial Kolmogorov-Smirnov and Berman's  $Z_2$  (Berman, 1986) statistics were used  
502 in order to test the dependence of the UB4c pattern on the covariate erosional sur-  
503 face. Both KS ( $D = 0.11952$ ,  $p - value = 7.772e - 16$ ) and  $Z_2$  ( $Z_2 = -7.8447$ ,  
504  $p - value = 4.34e - 15$ ) significantly rejected the null hypothesis of CSR. Although  
505 the tests suggested evidence that the intensity depends on the covariate, the effect of  
506 the covariate is weak and it seems to have no discriminatory power. The ROC curve  
507 and AUC statistics (0.56), which measure the strength of the covariate effect, suggest  
508 that the underlying UB4c/5a topography does not completely explain the localised high  
509 density of occurrence in the UB4c.

510 Relative spatial segregation seems to occur between the assemblages from UB4c  
511 (Fig. 10a) and UB5a (Fig. 10b), with high density of the former distribution corre-  
512 sponding to low density of the latter. The former analysis of the vertical distribution  
513 showed that the two assemblages occur very close to their stratigraphic contact. In  
514 order to further investigate the spatial interaction between the two depositional events,  
515 we applied multitype pair correlation ( $g_{ij}(r)$ ) and nearest-neighbour ( $G_{ij}(r)$ ) functions.

516 Fig. 10d shows the estimated values of the multivariate  $\hat{g}_{ij}(r)$  function against the  
517 envelope of the null hypothesis, obtained by randomly shifting the position of remains  
518 from the two distributions in 199 Monte Carlo simulations. For fixed values of  $r$  less

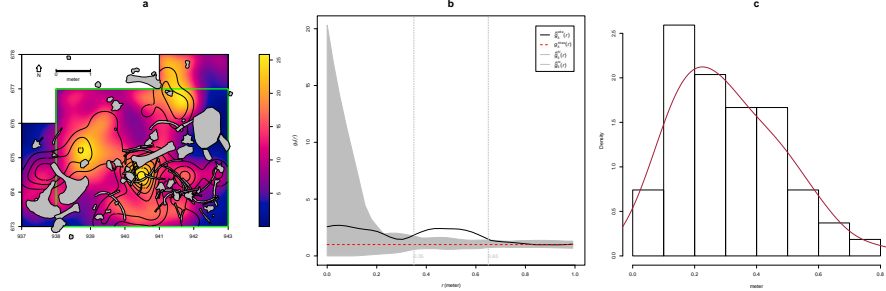


Figure 10: Kernel smoothed intensity function of the lithic and faunal assemblages from UB4c (a) and UB5a (b). Smoothing estimate of the intensity of remains from UB4c, as a function of the erosional surface UB4c/5a. Grey shading is pointwise 95% confidence bands (c). Cross-pattern pair correlation function ( $g_{ij}(r)$ ) between the UB4c and UB5a distributions. Grey envelope of 199 Monte Carlo simulations under the independence of components null hypothesis (d). Multitype nearest-neighbour function ( $G_{ij}(r)$ ) between the UB4c and UB5a distributions (e).

than 30 cm the observed function lies below the benchmark value of independence, thus indicating segregation; but it wanders at the lower edge of the grey envelope. For fixed distances of  $r > 0.3$  m the observed and theoretical lines significantly overlap. Overall, the function suggests independence of the two point processes (UB4c and UB5a) at multiple scales.

However, the estimated  $\hat{G}_{ij}(r)$  function (Fig. 10c), running well below the significance grey envelope for fixed values of  $r > 0.3$  m, confirms that the nearest-neighbour distances between remains from UB4c and UB5a are significantly longer than expected in the case of independent processes. Interestingly, at values of  $r < 0.2$  m the observed function failed to reject the null hypothesis of Complete Spatial Randomness and Independence (CSRI).

With the aim to integrate the vertical distribution analysis, the particle size spatial distribution of remains from the UB4c unit were investigated by means of a derivative of the multitype  $K$ -function, randomly labelling the classes of remains. Fig. 11 shows a selection of the array of possible combinations between classes. In any panel, the estimated function wanders above the benchmark value. Such positive deviations from the null hypotheses suggest that debris/chips are more likely to be found close to the other class of remains than would be expected in case of a completely random

537 distribution. Permutating the lithic debris/chips with flakes (Fig.11a), tools (Fig.11b),  
538 cores (Fig.11c) and faunal remains (Fig.11d), the Monte Carlo test results would have  
539 been significantly consistent with clustering, if we had chosen distance values  $r > 0.4$ ,  
540  $r > 0.4$ ,  $r > 0.9$ ,  $r > 0.8$ , respectively. Conversely, we could not reject the null  
541 hypothesis of CSRI for lesser values of  $r$ .

542 **5. Discussion**

543 Recent excavations at the Middle Pleistocene site of Marathousa 1 have unearthed  
544 in one of the two investigated areas (Area A) a partial skeleton of a single individual of  
545 *Elephas (P.) antiquus*, whose bones are in close anatomical association, and spatially  
546 and stratigraphically associated with lithic artefacts and other faunal remains. In Area  
547 B, 60 m to the South of Area A, we collected a much higher number of lithic artefacts  
548 (Tourloukis et al., this issue), spatially and stratigraphically associated with other fau-  
549 nal remains, including isolated elephant bones, cervids and carnivores among others  
550 (Konidaris et al., this issue).

551 The two areas are stratigraphically correlated, the main fossiliferous layers (UA3c  
552 and UB4c) representing a relatively low-energy depositional process, such as a hyper-  
553 concentrated flow that dumped material in a lake margin context (Karkanas et al., this  
554 issue).

555 To date, evidence of butchering (cut-marks) has been identified on two bones of  
556 the elephant skeleton from Area A, as well on elephant and other mammal bones from  
557 Area B (see Konidaris, this issue).

558 However, due to the secondary depositional nature of the main fossiliferous hori-  
559 zon, it is of primary importance to evaluate the degree and reliability of the spatial  
560 association of the lithic artefacts with the faunal remains, and especially with the ele-  
561 phant skeleton. In order to tackle our main objective, we applied a comprehensive  
562 set of spatial statistics to the distributions of the archaeological and zooarchaeologi-  
563 cal/palaeontological remains from relevant stratigraphic units of the two areas of in-  
564 vestigation. Results of our analyses are here discussed for both areas.

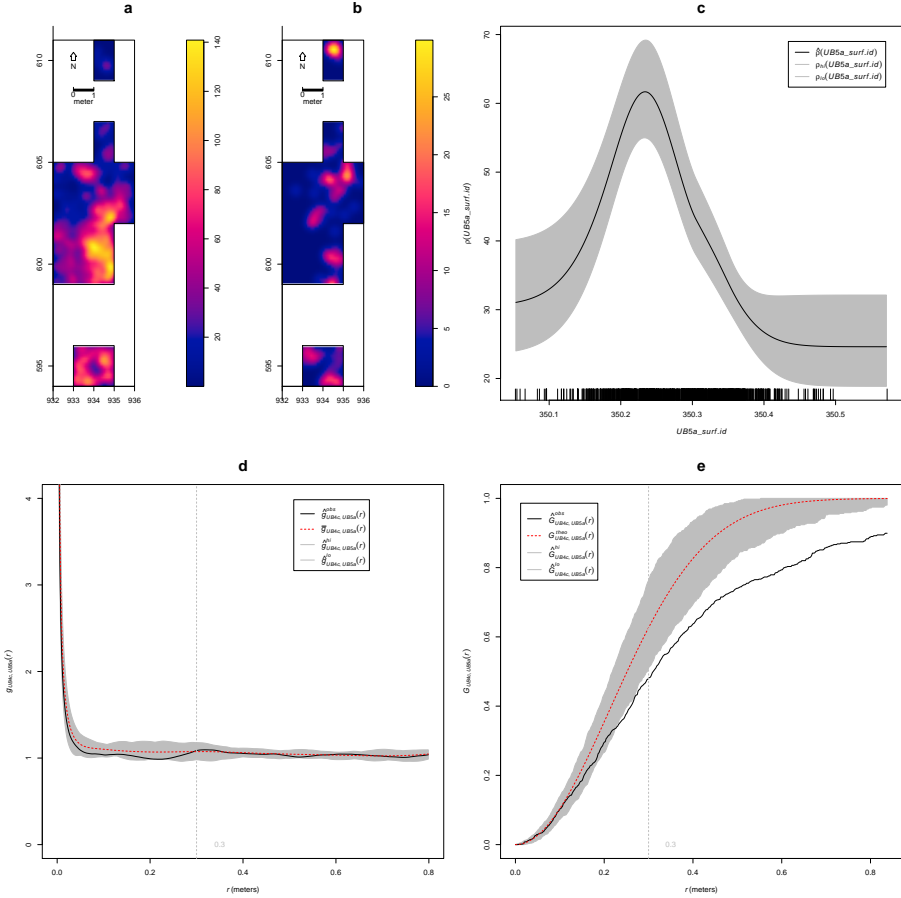


Figure 11: Random labelling test for the UB4c assemblage. Grey pointwise envelope of 199 Monte Carlo permutation of debris/chips with flakes (a); tools (b); cores (c); flakes/tools (d); fossils (e).

565     *5.1. Fabric analysis*

566     The analysis of the orientation (dip and strike) of subsets of remains, mostly bone  
567     fragments, organic residues and lithic artefacts, showed different patterns for the two  
568     main find-bearing units.

569     The test results (Tab. 3) for the UA4 sample and the sample of elephant remains  
570     - which lie on unit UA4 and are covered by UA3c - indicated significant preferential  
571     orientations towards the NE (Figs. 4b,c). As shown by the Woodcock's (Fig. 5) and the  
572     Benn's diagrams (Fig. 6), these samples plotted together at a distance from the others.  
573     Such convergence suggests that the elephant carcass, the other faunal remains and the  
574     organic material, deposited on unit UA4, were subject to the same processes.

575     Far from the isotropic corner in the Benn's diagram these two samples from Area  
576     A plotted approximately in between the linear and planar extremes, with the elephant  
577     sample showing a more planar fabric. When the results published by Bertran et al.  
578     (1997) and Lenoble and Bertran (2004) from observations of fabrics in modern sub-  
579     aerial slope deposits were used as a reference, the two samples aggregated well within  
580     the cluster of runoff process. Yet, they still plotted at the extreme margins of debris  
581     flow and relatively distant from the linear corner.

582     This result is consistent with the exposure of unit UA4 to overland water-laden  
583     processes that occurred before the flood event UA3/UB4 (Karkanas et al., this is-  
584     sue). Notably, the erosive nature of low-energy processes triggered by rain-water has  
585     been observed on lacustrine floodplains, and is associated with anisotropic patterns  
586     in autochthonous assemblages (Cobo-Sánchez et al., 2014; Domínguez-Rodrigo et al.,  
587     2014c; García-Moreno et al., 2016).

588     On the other hand, the fabric of the UA3c sample, being similar to those of the  
589     UB4c sub-samples (Figs. 5 and 6), supports the stratigraphic correlation between these  
590     units across the two investigated areas. The fabric analysis suggests that the UA3/UB4  
591     process can be categorized as a flood event, which falls in between the spectrum of de-  
592     bris and hyperconcentrated flow. Indeed, random distribution and orientation of clasts  
593     is expected for debris flows, except at flow margins, where preferential orientation and  
594     clusters of clasts have been observed (Pierson, 2005).

595     Unlike bones with a tubular shape (i.e., long bones), ribs and vertebrae are prone

596 to orient preferentially under high energy processes, less likely under low energy pro-  
597 cesses (Domínguez-Rodrigo and García-Pérez, 2013; Domínguez-Rodrigo et al., 2014c).  
598 Interestingly, whereas some of the ribs share the same preferential orientation with the  
599 long bones, others are oriented NW/SE. However, a NW/SE orientation could be con-  
600 sistent with a prevalent NE direction of the flow (and vice-versa), since long bones  
601 could roll orthogonally to the flow direction (Voorhies, 1966).

602 On the other hand, a higher energy flood would lead to an under-representation  
603 of most cancellous grease-bearing bones, which are prone to be easily transported by  
604 water induced processes (Voorhies, 1966). Yet several carpals, tarsals, metapodials,  
605 phalanges, ribs and vertebrae are present and in close spatial association with the ele-  
606 phant cranium and other skeletal elements.

607 The presence of many of the skeletal elements suggests that the elephant carcass  
608 was not subjected to high energy processes. Thus, we can assume that relatively low  
609 energy overland flows slightly reworked and oriented the exposed elements of the  
610 already dismembered (and probably already marginally displaced) elephant carcass,  
611 which mostly preserves close anatomical associations, but not anatomical connections.

612 In Area B, two sub-samples from the same stratigraphic unit were analysed, accord-  
613 ing to the different methods used for recording the orientation (dip and strike) of the  
614 finds (i.e., 'clock' vs. compass), mostly faunal remains, wood fragments and lithic arte-  
615 facts. Due to the different shapes of the two distributions (Figs. 4d,e), test statistics re-  
616 ported contrasting results (Tab. 3). Indeed, the clock system, recording non-continuous  
617 circular data, tends to produce a distribution more subject to show a multimodal shape  
618 when the distribution is actually uniform. However, the three-dimensional Woodcock  
619 (Fig. 5) and Benn (Fig. 6) diagrams agreed upon assessing the randomness of the sam-  
620 ples. Despite minor differences between the two samples, both plotted with the UA3c  
621 sample in the reference range of debris flows.

622 *5.2. Vertical distribution*

623 As for the vertical distribution, we assume that mass wasting processes, such as  
624 debris or hyperconcentrated flows, would predominantly distribute extremely poorly  
625 sorted clasts homogeneously throughout the sequence. Normal or inverse grading can

626 be observed in such flows (Pierson, 2005). A concentration of unsorted elements in the  
627 proximity of the erosional surface, as well as the absence of any grading, would in turn  
628 suggest an autochthonous assemblage.

629 The lithic assemblage from Area A - the combined sample from units UA3c and  
630 UA4 ( $n = 54$ ), composed by a few debitage products and a relatively high number of  
631 debris/chips and retouch waste products (Tab. 2) - plotted predominantly in the prox-  
632 imity of the erosional surface created by the UA3/UB4 event. The faunal remains  
633 from unit UA3c resemble the distribution of the archaeological assemblage as a whole;  
634 whereas the ones from the underlying unit UA4 match the vertical distribution of the  
635 elephant (Fig. 7).

636 Overall, the material recovered from unit UA3c did not show any grading and  
637 mainly plotted at the bottom of the unit, thus is consistent with the hypothesis of an  
638 autochthonous assemblage.

639 In Area B, two samples from units UB4c ( $n = 1243$ ) and UB5a ( $n = 101$ ) respec-  
640 tively, were analysed (Tab. 2) for quantifying the minimum orthogonal distance of each  
641 item to the modelled erosional surface (Fig. 3b).

642 The vertical distribution of lithic artefacts and fossils from unit UB4c showed a pre-  
643 dominant peak right at the contact with the erosional surface. Almost 30% of this rich  
644 sample plotted at a distance between 0 and 5 cm from the erosional contact; whereas  
645 the rest gently skewed to the upper part of the unit, up to about 50 cm. The same distri-  
646 bution was observed for all classes of remains, suggesting no size sorting and an origin  
647 very close to the erosional surface (Fig. 8b).

648 The density distribution of the sample from the underlying UB5a unit (Fig. 8a)  
649 globally indicates a more constrained vertical displacement of remains (within 30 cm  
650 below the erosional surface). Whereas lithic artefacts and fossils mostly plot right at  
651 the contact and just below it, a few debris/chips and faunal remains were found lower  
652 in the sequence. No size sorting was observed, but, notably, lithic cores are absent and  
653 the debris/chip distribution is wider than the distribution of the few flakes and tools.

654 Field observations of cracks in the clayey UB5a unit testify to shrinking and swelling  
655 during wet and dry cycles (Karkanas et al., this issue), which suggests that vertical dis-  
656 placement of some small lithics and fossil fragments at lower depths with respect to

657 the UB5a/4c contact probably resulted from clay desiccation.

658 Likewise, [Lenoble and Bertran \(2004\)](#) documented up to 30 cm vertical dispersion  
659 and frequent vertical dip of artefacts from the marshy silty clay of the Croix-de-Canard  
660 site, sector 3.

661 Furthermore, a recent experimental study of animal trampling in water saturated  
662 substrates reported negative correlation with artefact size, significant inclination and  
663 greater vertical displacement than any former work: a maximum between 16 and  
664 21 cm, with a mean of about 6 cm ([Eren et al., 2010](#)).

665 The fact that the majority of the remains from units UB4c and UB5a plotted at,  
666 or very close to the contact between these two layers, the relatively high percentage  
667 of lithics in both units, as well as the absence of size sorting or grading, suggest au-  
668 tochthonous assemblages, deposited in UB5a and subsequently eroded *in situ* by the  
669 UA3/UB4 flood event.

670 *5.3. Point pattern analysis*

671 The hypothesis that in both areas the lithic and faunal assemblages were primarily  
672 deposited *in situ* and were subsequently reworked by a low energy flood, was further  
673 explored by means of point pattern analysis.

674 We assumed that a completely random spatial distribution of the lithic artefacts  
675 and faunal remains would suggest an allochthonous origin and subsequent transport to  
676 the site by the action of a random massive process, such as debris flow. Nevertheless,  
677 clustering of artefacts is not necessarily evidence of human presence. Aggregation or  
678 segregation patterns could be produced by a range of biotic and/or natural processes.  
679 Human activities, topography and physical obstructions alike could trigger spatial ag-  
680 gregation.

681 The three-dimensional distribution of lithic artefacts from unit UA3c shows signif-  
682 icant clustering for values of  $r$  between 35 and 65 cm. Lithic artefacts occur relatively  
683 close to the skeletal elements of the elephant, at a distance between 20 and 50 cm at  
684 most (Fig. 9). The richest cluster of about 20 lithic artefacts is located to the SW of the  
685 cranium, close to the right femur and the scatter of ribs and vertebrae.

686 Considering the prevalent NE orientation of the elephant bones and the other fau-  
687 nal remains from UA4, it is not unlikely that a SW/NE oriented flood could have been  
688 responsible for the observed accumulation to the SW of the elephant cranium, which  
689 would have represented an important obstruction to the flow. A similar case of clus-  
690 tering of small remains, apparently dammed by a long elephant tusk, has also been  
691 observed at Castel di Guido (Italy) ([Boschian and Saccà, 2010](#)). Secondary deposi-  
692 tion by low-energy flows and clustering of artefacts and bones blocked by an aurochs  
693 carcass have been as well documented at the site of 'Ein Qashishadd (Israel) (?).

694 As mentioned above, whereas fairly random fabric and spatial distribution of coarse  
695 clasts are observed at the centre of modern debris flow deposits, preferential orientation  
696 and clustering may occur at the margin of the flood ([Pierson, 2005](#)). Yet the fabric  
697 analysis of the UA3c sample shows a random distribution, which falls within the range  
698 of debris flow (Fig. 6), and the pair correlation function (Fig. 9b) suggests significant  
699 clustering of lithic artefacts at relatively small scale: a pattern less likely to be produced  
700 by a large scale massive process such as a debris flow. Moreover, clusters of lithic  
701 artefacts occur as well in areas with lower densities of elephant bones.

702 Small scale clustering; proximity to the elephant remains and the erosional surface;  
703 absence of spatial size sorting and, on the contrary, the presence of a relatively high  
704 number of lithic debris/chips associated with some flakes and tools; close anatomical  
705 spatial association of the elephant skeletal elements, slightly displaced and preferen-  
706 tially oriented: these lines of evidences support the hypothesis of an autochthonous  
707 deposition, subject to localised minor reworking.

708 A similar pattern can be observed in Area B, where an initial set of spatial statistics  
709 confirmed that the inhomogeneous density of remains from unit UB4c (Fig. 10a) is  
710 not completely explained by the covariate effect of the underlying complex topography  
711 created by the erosional event UA3/UB4 (Fig. 3b).

712 Thus, we explored the relative spatial interaction between the UB4c and the un-  
713 derlying UB5a samples. We assumed that complete spatial randomness of the two  
714 independent depositional processes would occur in case of an exogenous origin and  
715 transportation of the UB4c assemblage. The hypothesis of an autochthonous original  
716 deposition of the faunal and lithic assemblages on the UB5a unit, subsequently eroded

717 *in situ* by a relatively high energy flood (UB4c), was tested by cross-pattern spatial  
718 correlation functions (Figs. 10d,e). Whereas the two samples are vertically adjacent to  
719 the erosional surface (Fig. 8), on the horizontal plane they are both more segregated  
720 than expected for a random distribution.

721 Moreover, for the UB4c sample, an unsorted particle size spatial distribution was  
722 confirmed (Fig. 11). The occurrence in the same place of small and large classes of  
723 remains suggests that post-depositional processes, such as water winnowing, have not  
724 severely affected the assemblage. Hyperconcentrated flows would have dumped mate-  
725 rial onto the lake margin. In this way, particles would have been frozen and deposited  
726 *en masse*. Hence their non-sorted spatial distribution.

727 Conversely, the extraordinary preservation and number of mint to sharp, unsorted  
728 lithic artefacts from the UB4c unit; their density, positively correlated to the topog-  
729 raphy, and significantly segregated from the underlying distribution of remains; the  
730 vertical proximity of both assemblages from UB4c and UB5a to the erosional surface;  
731 as well as the random orientation pattern of the former, suggest that significant dis-  
732 placement of materials due to the erosional event can be excluded.

733 The faunal and lithic assemblages from unit UB4c therefore most likely derived  
734 from the local erosion of exposed mudflat areas (UB5a layer) and have been slightly  
735 redistributed by the same flood event that capped the elephant in Area A.

736 Further evidence that the recovered assemblage has not undergone substantial re-  
737 working and has retained its original characteristics would come from the refitting anal-  
738 ysis, currently in progress. To date, 4 bone refits have been found in Area B: three from  
739 unit UB4c, respectively at 4.77, 0.05 and 0.01 m distance; and one between two mam-  
740 mal bone fragments from units UB4c and UB5a, at a very short distance (0.09 m).  
741 Interestingly, one of the elements of the most distant refit (a *Dama sp.* mandibular  
742 fragment) shows traces of carnivore gnawing (Konidaris et al., this issue).

743 In conclusion, multiple lines of evidence suggest that the erosional event UB4/UA3  
744 represents a relatively low-energy process in the continuum between debris and hyper-  
745 concentrated flow, which would have locally reworked at a small scale the already  
746 exposed or slightly buried and spatially associated lithic and faunal assemblages.

747 Although the UB4/UA3 process represents a snapshot of a relatively short time-

748 frame, inferences about the use of space by human groups, in terms of knapping  
749 episodes and butchering activities, are unreliable in light of the current information.

750 The spatial pattern observed at the site is indeed the result of the last episode in  
751 a palimpsest of spatial processes. Whereas the erosional event represented by the de-  
752 bris/hyperconcentrated flow UA3/UB4 caps the sequence and preserves the record, lit-  
753 tle is known about the eroded underlying occupational horizon.

754 However, whereas hunting or scavenging is still an unsolved matter of debate, con-  
755 sidering the rate of bone fragmentation, the density of lithic debris/chips, the number  
756 of processed bones and their spatial density and association, it is likely that the assem-  
757 blage represents a complex palimpsest of locally repeated events of hunting/scavenging  
758 and exploitation of lake shore resources.

759 More data from high resolution excavations in the coming years will allow us to  
760 refine the coarse-grained spatio-temporal resolution of our inferences about past human  
761 behaviour at Marathousa 1.

## 762 **6. Conclusions**

763 At the Middle Pleistocene open-air site of Marathousa 1, a partial skeleton of a  
764 single individual of *Elephas (Palaeoloxodon) antiquus* was recovered in stratigraphic  
765 association with a rich and consistent lithic assemblage and other vertebrate remains.  
766 Cut-marks and percussion marks have been identified on the elephant and other mam-  
767 mal bones excavated at the site. The main find-bearing horizon represents a secondary  
768 depositional process in a lake margin context.

769 Understanding the site formation processes is of primary importance in order to  
770 reliably infer hominin exploitation of the elephant carcass and other animals. To meet  
771 this aim, we applied a comprehensive set of multivariate and multiscale spatial analyses  
772 in a taphonomic framework.

773 Results from the fabric, vertical distribution and point pattern analyses are consis-  
774 tent with a relatively low-energy erosional process slightly reworking at a small scale  
775 an exposed (or slightly buried) and consistent scatter of lithic artefacts and faunal re-  
776 mains. These results are in agreement with preliminary taphonomic observations of

777 the lithic artefacts (Tourloukis et al., this issue) and the faunal remains (Konidaris et  
778 al., this issue), which also indicate minor weathering and transportation. Our analyses  
779 show that multiple lines of evidence support an autochthonous origin of the lithic and  
780 faunal assemblages, subject to minor post-depositional reworking. Human activities  
781 therefore took place on-site, during an as of yet uncertain range of time.

782 **Acknowledgements**

783 This research is supported by the European Research Council (ERC StG PaGE  
784 283503) awarded to K. Harvati. We are grateful to the Municipality of Megalopolis,  
785 the authorities of the Region of Peloponnese, and the Greek Public Power corporation  
786 ( $\Delta$ EH) for their support. We also thank Julian Bega and all the participants in the PaGE  
787 survey and excavation campaigns in Megalopolis for their indispensable cooperation.

788 **References**

- 789 Anderson, K. L., Burke, A., 2008. Refining the definition of cultural levels at Karabi  
790 Tamchin: a quantitative approach to vertical intra-site spatial analysis. *Journal of  
791 Archaeological Science* 35 (8), 2274–2285.
- 792 Baddeley, A., Chang, Y.-M., Song, Y., Turner, R., 2012. Nonparametric estimation of  
793 the dependence of a point process on spatial covariates. *Statistics and Its Interface*  
794 5 (2), 221–236.
- 795 Baddeley, A., Rubak, E., Turner, R., 2015. *Spatial Point Patterns: Methodology and  
796 Applications* with R. Chapman and Hall/CRC, London.
- 797 Bar-Yosef, O., Tchernov, E., 1972. On the palaeo-ecological history of the site of Ubei-  
798 diya. Vol. 35. Israel Academy of Sciences and Humanities, Jerusalem.
- 799 Bargalló, A., Gabucio, M. J., Rivals, F., 2016. Puzzling out a palimpsest: Testing  
800 an interdisciplinary study in level o of abric romaní. *Quaternary International*  
801 417 (Supplement C), 51 – 65, advances in Palimpsest Dissection.
- 802 URL [http://www.sciencedirect.com/science/article/pii/  
803 S1040618215009635](http://www.sciencedirect.com/science/article/pii/S1040618215009635)

- 804 Benito-Calvo, A., de la Torre, I., 2011. Analysis of orientation patterns in Olduvai  
805 Bed I assemblages using GIS techniques: Implications for site formation processes.  
806 *Journal of Human Evolution* 61 (1), 50 – 60.
- 807 Benito-Calvo, A., Martínez-Moreno, J., Mora, R., Roy, M., Roda, X., 2011. Trampling  
808 experiments at Cova Gran de Santa Linya, Pre-Pyrenees, Spain: their relevance for  
809 archaeological fabrics of the Upper–Middle Paleolithic assemblages. *Journal of Ar-  
810 chaeological Science* 38 (12), 3652–3661.
- 811 Benito-Calvo, A., Martínez-Moreno, J., Pardo, J. F. J., de la Torre, I., Torcal, R. M.,  
812 2009. Sedimentological and archaeological fabrics in Palaeolithic levels of the  
813 South-Eastern Pyrenees: Cova Gran and Roca dels Bous Sites (Lleida, Spain). *Jour-  
814 nal of Archaeological Science* 36 (11), 2566 – 2577.
- 815 Benn, D., 1994. Fabric shape and the interpretation of sedimentary fabric data. *Journal  
816 of Sedimentary Research* 64 (4a), 910–915.
- 817 Berman, M., 1986. Testing for spatial association between a point process and another  
818 stochastic process. *Applied Statistics* 35, 54–62.
- 819 Bernatchez, J. A., 2010. Taphonomic implications of orientation of plotted finds from  
820 Pinnacle Point 13B (Mossel Bay, Western Cape Province, South Africa). *Journal of  
821 Human Evolution* 59 (3–4), 274 – 288.
- 822 Bertran, P., Hetù, B., Texier, J.-P., Steijn, H. V., 1997. Fabric characteristics of subaerial  
823 slope deposits. *Sedimentology* 44 (1), 1 – 16.
- 824 Bertran, P., Lenoble, A., Todisco, D., Desrosiers, P. M., Sørensen, M., 2012. Particle  
825 size distribution of lithic assemblages and taphonomy of Palaeolithic sites. *Journal  
826 of Archaeological Science* 39 (10), 3148 – 3166.
- 827 Bertran, P., Texier, J.-P., 1995. Fabric Analysis: Application to Paleolithic Sites. *Jour-  
828 nal of Archaeological Science* 22 (4), 521 – 535.
- 829 Bevan, A., Crema, E., Li, X., Palmisano, A., 2013. Intensities, Interactions, and Un-  
830 certainties: Some New Approaches to Archaeological Distributions. In: Bevan, A.,

- 831 Lake, M. (Eds.), Computational Approaches to Archaeological Spaces. Left Coast  
832 Press, Walnut Creek, pp. 27–52.
- 833 Boschian, G., Saccà, D., 2010. Ambiguities in human and elephant interactions? Sto-  
834 ries of bones, sand and water from Castel di Guido (Italy). Quaternary International  
835 214 (1–2), 3 – 16.
- 836 Carrer, F., 2015. Interpreting Intra-site Spatial Patterns in Seasonal Contexts: an Eth-  
837 noarchaeological Case Study from the Western Alps. Journal of Archaeological  
838 Method and Theory, 1–25.
- 839 Clark, A. E., 2016. Time and space in the middle paleolithic: Spatial structure and  
840 occupation dynamics of seven open-air sites. Evolutionary Anthropology: Issues,  
841 News, and Reviews 25 (3), 153–163.
- 842 Cobo-Sánchez, L., Aramendi, J., Domínguez-Rodrigo, M., 2014. Orientation patterns  
843 of wildebeest bones on the lake Masek floodplain (Serengeti, Tanzania) and their  
844 relevance to interpret anisotropy in the Olduvai lacustrine floodplain. Quaternary  
845 International 322–323 (0), 277 – 284.
- 846 de la Torre, I., Benito-Calvo, A., 2013. Application of GIS methods to retrieve ori-  
847 entation patterns from imagery; a case study from Beds I and II, Olduvai Gorge  
848 (Tanzania). Journal of Archaeological Science 40 (5), 2446–2457.
- 849 Diggle, P., 1985. A kernel method for smoothing point process data. Applied Statistics  
850 (Journal of the Royal Statistical Society, Series C) 34, 138–147.
- 851 Domínguez-Rodrigo, M., Bunn, H., Mabulla, A., Baquedano, E., Uribelarrea, D.,  
852 Pérez-González, A., Gidna, A., Yravedra, J., Diez-Martin, F., Egeland, C., Barba,  
853 R., Arriaza, M., Organista, E., Ansón, M., 2014a. On meat eating and human evolu-  
854 tion: A taphonomic analysis of BK4b (Upper Bed II, Olduvai Gorge, Tanzania), and  
855 its bearing on hominin megafaunal consumption. Quaternary International 322–323,  
856 129–152.
- 857 Domínguez-Rodrigo, M., Bunn, H., Pickering, T., Mabulla, A., Musiba, C., Baque-  
858 dano, E., Ashley, G., Diez-Martin, F., Santonja, M., Uribelarrea, D., Barba, R.,

- 859 Yravedra, J., Barboni, D., Arriaza, C., Gidna, A., 2012. Autochthony and orientation  
860 patterns in Olduvai Bed I: a re-examination of the status of post-depositional biasing  
861 of archaeological assemblages from FLK North (FLKN). *Journal of Archaeological*  
862 *Science* 39 (7), 2116 – 2127.
- 863 Domínguez-Rodrigo, M., Cobo-Sánchez, L., Yravedra, J., Uribelarrea, D., Arriaza, C.,  
864 Organista, E., Baquedano, E., 2017. Fluvial spatial taphonomy: a new method for the  
865 study of post-depositional processes. *Archaeological and Anthropological Sciences*,  
866 1–21.
- 867 Domínguez-Rodrigo, M., Diez-Martín, F., Yravedra, J., Barba, R., Mabulla, A., Baque-  
868 dano, E., Uribelarrea, D., Sánchez, P., Eren, M. I., 2014b. Study of the SHK Main  
869 Site faunal assemblage, Olduvai Gorge, Tanzania: Implications for Bed II taphon-  
870 omy, paleoecology, and hominin utilization of megafauna. *Quaternary International*  
871 322–323, 153–166.
- 872 Domínguez-Rodrigo, M., García-Pérez, A., 07 2013. Testing the Accuracy of Different  
873 A-Axis Types for Measuring the Orientation of Bones in the Archaeological and  
874 Paleontological Record. *PLoS ONE* 8 (7), e68955.
- 875 Domínguez-Rodrigo, M., Uribelarrea, D., Santonja, M., Bunn, H., García-Pérez, A.,  
876 Pérez-González, A., Panera, J., Rubio-Jara, S., Mabulla, A., Baquedano, E., Yrave-  
877 dra, J., Diez-Martín, F., 2014c. Autochthonous anisotropy of archaeological mate-  
878 rials by the action of water: experimental and archaeological reassessment of the  
879 orientation patterns at the Olduvai sites . *Journal of Archaeological Science* 41 (0),  
880 44 – 68.
- 881 Eren, M. I., Durant, A., Neudorf, C., Haslam, M., Shipton, C., Bora, J., Korisettar,  
882 R., Petraglia, M., 2010. Experimental examination of animal trampling effects on  
883 artifact movement in dry and water saturated substrates: a test case from South India.  
884 *Journal of Archaeological Science* 37 (12), 3010 – 3021.
- 885 Gabucio, M. J., Fernández-Laso, M. C., Rosell, J., 2017. Turning a rock shelter into a  
886 home. neanderthal use of space in abric romaní levels m and o. *Historical Biology*

- 887 0 (0), 1–24.
- 888 URL <http://dx.doi.org/10.1080/08912963.2017.1340470>
- 889 García-Moreno, A., Smith, G. M., Kindler, L., Pop, E., Roebroeks, W., Gaudzinski-  
890 Windheuser, S., Klinkenberg, V., 2016. Evaluating the incidence of hydrological  
891 processes during site formation through orientation analysis. A case study of the  
892 middle Palaeolithic Lakeland site of Neumark-Nord 2 (Germany). *Journal of Ar-  
893 chaeological Science: Reports* 6, 82 – 93.
- 894 Gifford-Gonzalez, D., Damrosch, D., Damrosch, D., Pryor, J., Thunen, R., 1985. The  
895 Third Dimension in Site Structure: An Experiment in Trampling and Vertical Dis-  
896 persal. *American Antiquity* 50 (4), 803–818.
- 897 Giusti, D., Arzarello, M., 2016. The need for a taphonomic perspective in spatial analy-  
898 sis: Formation processes at the Early Pleistocene site of Pirro Nord (P13), Apricena,  
899 Italy. *Journal of Archaeological Science: Reports* 8, 235 – 249.
- 900 Harvati, K., Panagopoulou, E., Tourloukis, V., Thompson, N., Karkanas, P., Athanas-  
901 siou, A., Konidaris, G., Tsartsidou, G., Giusti, D., 2016. New Middle Pleistocene  
902 elephant butchering site from Greece. In: Paleoanthropology Society Meeting. At-  
903 lanta, Georgia, pp. A14–A15.
- 904 Hivernel, F., Hodder, I., 1984. Analysis of artifact distribution at Ngenyem (Kenya):  
905 depositional and postdepositional effects. In: Hietala, H., Larson, P. (Eds.), *Intrasite*  
906 *Spatial Analysis in Archaeology*. Cambridge University Press, Ch. 7, pp. 97–115.
- 907 Hodder, I., Orton, C., 1976. *Spatial Analysis in Archaeology. New Studies in Archae-  
908 ology*. Cambridge University Press, Cambridge.
- 909 Isaac, G. L., 1967. Towards the interpretation of occupation debris: Some experiments  
910 and observations. *Kroeber Anthropological Society Papers* 37 (37), 31–57.
- 911 Jammalamadaka, S., Sengupta, A., Sengupta, A., 2001. *Topics in Circular Statistics.  
912 Series on multivariate analysis*. World Scientific.

- 913 Lenoble, A., 2005. Ruissellement et formation des sites préhistoriques. Référentiel ac-  
914 tualiste et exemple d'application au fossile. Vol. 1363 of International Series. British  
915 Archaeological Report, Oxford.
- 916 Lenoble, A., Bertran, P., 2004. Fabric of Palaeolithic levels: methods and implications  
917 for site formation processes. *Journal of Archaeological Science* 31 (4), 457 – 469.
- 918 Lenoble, A., Bertran, P., Lacrampe, F., 2008. Solifluction-induced modifications  
919 of archaeological levels: simulation based on experimental data from a modern  
920 periglacial slope and application to French Palaeolithic sites. *Journal of Archaeo-*  
921 *logical Science* 35 (1), 99 – 110.
- 922 López-Ortega, E., Bargalló, A., de Lombera-Hermida, A., Mosquera, M., Ollé, A.,  
923 Rodríguez-Álvarez, X. P., 2015. Quartz and quartzite refits at Gran Dolina (Sierra  
924 de Atapuerca, Burgos): Connecting lithic artefacts in the Middle Pleistocene unit of  
925 TD10.1. *Quaternary International*, –.
- 926 López-Ortega, E., Rodríguez, X. P., Vaquero, M., 2011. Lithic refitting and movement  
927 connections: the NW area of level TD10-1 at the Gran Dolina site (Sierra de Ata-  
928 puerca, Burgos, Spain). *Journal of Archaeological Science* 38 (11), 3112 – 3121.
- 929 Malinsky-Buller, A., Hovers, E., Marder, O., 2011. Making time: ‘Living floors’,  
930 ‘palimpsests’ and site formation processes – A perspective from the open-air Lower  
931 Paleolithic site of Revadim Quarry, Israel. *Journal of Anthropological Archaeology*  
932 30 (2), 89 – 101.
- 933 URL [http://www.sciencedirect.com/science/article/pii/  
934 S0278416510000632](http://www.sciencedirect.com/science/article/pii/S0278416510000632)
- 935 Marwick, B., 2017. Computational reproducibility in archaeological research: Ba-  
936 sic principles and a case study of their implementation. *Journal of Archaeological  
937 Method and Theory* 24 (2), 424–450.
- 938 McPherron, S. J., 2005. Artifact orientations and site formation processes from total  
939 station proveniences. *Journal of Archaeological Science* 32 (7), 1003 – 1014.

- 940 Morin, E., Tsanova, T., Sirakov, N., Rendu, W., Mallye, J.-B., Lèveque, F., 2005. Bone  
941 refits in stratified deposits: testing the chronological grain at Saint-Cesaire. *Journal*  
942 of Archaeological Science 32, 1083–1098.
- 943 Morton, A. G. T., 2004. *Archaeological Site Formation: Understanding Lake Margin*  
944 *Contexts*. No. 1211 in BAR International Series. Archaeopress, Oxford.
- 945 Nickel, B., Riegel, W., Schonherr, T., Velitzelos, E., 1996. Environments of coal forma-  
946 tion in the Pleistocene lignite at Megalopolis, Peloponnesus (Greece) - reconstruc-  
947 tion from palynological and petrological investigations. *N. Jb. Geol. Palaont. A.* 200,  
948 201–220.
- 949 Nielsen, A. E., 1991. Trampling the archaeological record: an experimental study.  
950 *American Antiquity* 56 (3), 483–503.
- 951 Ohser, J., 1983. On estimators for the reduced second moment measure of point pro-  
952 cesses. *Mathematische Operationsforschung und Statistik, series Statistics* 14, 63–  
953 71.
- 954 Organista, E., Domínguez-Rodrigo, M., Yravedra, J., Uribelarrea, D., Arriaza, M. C.,  
955 Ortega, M. C., Mabulla, A., Gidna, A., Baquedano, E., 2017. Biotic and abiotic pro-  
956 cesses affecting the formation of BK Level 4c (Bed II, Olduvai Gorge) and their bear-  
957 ing on hominin behavior at the site. *Palaeogeography, Palaeoclimatology, Palaeo-  
958 ecology*, –.
- 959 Orton, C., 1982. Stochastic process and archaeological mechanism in spatial analysis.  
960 *Journal of Archaeological Science* 9 (1), 1 – 23.
- 961 Panagopoulou, E., Tourloukis, V., Thompson, N., Athanassiou, A., Tsartsidou, G.,  
962 Konidaris, G., Giusti, D., Karkanas, P., Harvati, K., 2015. Marathousa 1: a new Mid-  
963 dle Pleistocene archaeological site from Greece. *Antiquity Project Gallery* 89 (343).
- 964 Petraglia, M. D., Nash, D. T., 1987. The impact of fluvial processes on experimen-  
965 tal sites. In: Nash, D. T., Petraglia, M. D. (Eds.), *Natural formation processes and*  
966 *the archaeological record*. Vol. 352 of International Series. British Archaeological  
967 Reports, Oxford, pp. 108–130.

- 968 Petraglia, M. D., Potts, R., 1994. Water Flow and the Formation of Early Pleistocene  
969 Artifact Sites in Olduvai Gorge, Tanzania . Journal of Anthropological Archaeology  
970 13 (3), 228 – 254.
- 971 Pierson, T. C., 2005. Distinguishing between debris flows and floods from field evi-  
972 dence in small watersheds. Usgs numbered series, U.S. Geological Survey.
- 973 R Core Team, 2016. R: A Language and Environment for Statistical Computing. R  
974 Foundation for Statistical Computing, Vienna, Austria.
- 975 Rick, J. W., 1976. Downslope movement and archaeological intrasite spatial analysis.  
976 American Antiquity 41 (2), 133–144.
- 977 Ripley, B., 1977. Modelling spatial patterns. Journal of the Royal Statistical Society,  
978 series B 39, 172–212.
- 979 Ripley, B., 1988. Statistical inference for spatial processes. Cambridge University  
980 Press.
- 981 Ripley, B. D., 1976. The second-order analysis of stationary point processes. Journal  
982 of Applied Probability 13 (2), 255–266.
- 983 Ripley, B. D., 1981. Spatial Statistics. John Wiley and Sons, New York.
- 984 Schick, K. D., 1984. Processes of paleolithic site formation: an experimental study.  
985 Ph.D. thesis, University of California, Berkeley.
- 986 Schick, K. D., 1986. Stone Age sites in the making: experiments in the formation  
987 and transformation of archaeological occurrences. Vol. 319 of International Series.  
988 British Archaeological Reports, Oxford.
- 989 Schick, K. D., 1987. Modeling the formation of Early Stone Age artifact concentra-  
990 tions. Journal of Human Evolution 16, 789–807.
- 991 Schiffer, M. B., 1972. Archaeological Context and Systemic Context. American Antiq-  
992 uity 37 (2), 156–165.

- 993 Schiffer, M. B., 1983. Toward the identification of formation processes. *American An-*  
994 *tiquity* 48 (4), 675–706.
- 995 Schiffer, M. B., 1987. Formation processes of the archaeological record. University of  
996 New Mexico Press, Albuquerque.
- 997 Shackley, M. L., 1978. The behaviour of artefacts as sedimentary particles in a fluvialite  
998 environment. *Archaeometry* 20 (1), 55–61.
- 999 Sisk, M. L., Shea, J. J., 2008. Intrasite spatial variation of the Omo Kibish Middle Stone  
1000 Age assemblages: Artifact refitting and distribution patterns . *Journal of Human*  
1001 *Evolution* 55 (3), 486 – 500.
- 1002 Sánchez-Romero, L., Benito-Calvo, A., Pérez-González, A., Santonja, M., 12 2016.  
1003 Assessment of Accumulation Processes at the Middle Pleistocene Site of Ambrona  
1004 (Soria, Spain). Density and Orientation Patterns in Spatial Datasets Derived from  
1005 Excavations Conducted from the 1960s to the Present. *PLOS ONE* 11 (12), 1–27.
- 1006 Todd, L., Stanford, D., 1992. Application of conjoined bone data to site structural  
1007 studies. In: Hofman, J., Enloe, J. (Eds.), *Piecing Together the Past: Applications of*  
1008 *Refitting Studies in Archaeology*. Vol. 578 of International Series. BAR, Oxford, pp.  
1009 21–35.
- 1010 van Vugt, N., de Bruijn, H., van Kolfschoten, M., Langereis, C. G., 2000. Magneto-  
1011 and cyclostratigraphy and mammal-fauna's of the Pleistocene lacustrine Megalopo-  
1012 lis Basin, Peloponnesos, Greece. *Geologica Ultrajectina* 189, 69–92.
- 1013 Vaquero, M., Bargalló, A., Chacón, M. G., Romagnoli, F., Sañudo, P., 2015. Lithic re-  
1014 cycling in a Middle Paleolithic expedient context: Evidence from the Abric Romaní  
1015 (Capellades, Spain). *Quaternary International* 361, 212 – 228.
- 1016 Vaquero, M., Chacón, M. G., García-Antón, M. D., de Soler, B. G., Martínez, K.,  
1017 Cuartero, F., 2012. Time and space in the formation of lithic assemblages: The  
1018 example of Abric Romaní Level J. *Quaternary International* 247 (0), 162 – 181.

- 1019 Villa, P., 1982. Conjoinable Pieces and Site Formation Processes. *American Antiquity*  
1020 47 (2), 276–290.
- 1021 Villa, P., 1990. Torralba and Aridos: elephant exploitation in Middle Pleistocene Spain.  
1022 *Journal of Human Evolution* 19 (3), 299 – 309.
- 1023 Villa, P., Courtin, J., 1983. The interpretation of stratified sites: A view from under-  
1024 ground. *Journal of Archaeological Science* 10 (3), 267–281.
- 1025 Voorhies, M., 1966. Taphonomy and population dynamics of an early Pliocene verte-  
1026 brate fauna, Knox County, Nebraska. Ph.D. thesis, University of Wyoming.
- 1027 Walter, M. J., Trauth, M. H., 2013. A {MATLAB} based orientation analysis of  
1028 acheulean handaxe accumulations in olorgesailie and kariandusi, kenya rift. *Jour-*  
1029 *nal of Human Evolution* 64 (6), 569 – 581.
- 1030 Wood, R. W., Johnson, D. L., 1978. A survey of disturbance processes in archaeologi-  
1031 cal site formation. In: Schiffer, M. B. (Ed.), *Advances in archaeological method and*  
1032 *theory*. Vol. 1. Academic Press, Ch. 9, pp. 315–381.
- 1033 Woodcock, N., Naylor, M., 1983. Randomness testing in three-dimensional orientation  
1034 data. *Journal of Structural Geology* 5 (5), 539 – 548.